Electroelastic Response of Isotropic Dielectric Elastomer Composites with Deformation-Dependent Apparent-Permittivity Matrix

Victor Lefèvre
Department of Mechanical Engineering,
Northwestern University,
Evanston, IL 60208
e-mail: victor.lefevre@northwestern.edu

This paper puts forth an approximate yet accurate free energy for the elastic dielectric response—under finite deformations and finite electric fields—of non-percolative dielectric elastomer composites made out of a non-Gaussian dielectric elastomer matrix with deformation-dependent apparent permittivity isotropically filled with nonlinear elastic dielectric particles that may exhibit polarization saturation. While the proposed free energy applies in its most general form to arbitrary isotropic non-percolative microstructures, closed-form specializations are recorded for the practically relevant cases of rigid or liquid-like spherical particles. The proposed free energy is exact by construction in the asymptotic context of small deformations and moderate electric fields and is shown to remain accurate for arbitrary large deformations and electric fields via comparisons with full-field finite-element simulations. The proposed constitutive model is deployed to probe the electrostriction response of these dielectric elastomer composites and corresponding results reveal that their elastic dielectric response strongly depends on the deformation-dependent apparent permittivity of the matrix they comprise. [DOI: 10.1115/1.4047289]

Keywords: electrostriction, electroactive materials, dielectric elastomer composites, constitutive modeling of materials, micromechanics

1 Introduction and Main Results

Dielectric elastomers have been identified over the past 20 years as potential enablers of various new technologies ranging from artificial muscles for soft robotics to energy harvesters and Braille tactile displays [1–5]. As a result, these stretchable dielectrics received a lot of experimental attention to determine their electromechanical response when undergoing finite deformations while being subjected to finite electric fields. Experimental evidence [6–9] suggests that dielectric elastomers are so-called isotropic *ideal* dielectrics, that is, isotropic deformable dielectrics wherein the relation between the Eulerian electric displacement $\mathbf{d}$ and the Eulerian electric field $\mathbf{e}$ is linear,

$$\mathbf{d} = \boldsymbol{\varepsilon}_{\mathrm{m}}\mathbf{e} \quad \text{with } \boldsymbol{\varepsilon}_{\mathrm{m}} = \varepsilon_{\mathrm{m}}\mathbf{I} \tag{1}$$

and that *irrespectively* of the deformations and electric fields the material is subjected to. This being true in particular when the material is undeformed and subjected to small electric fields, the constant second-order tensor $\boldsymbol{\varepsilon}_{\mathrm{m}}$—and by extension, the constant material coefficient ε_{m}—in Eq. (1) can be naturally identified with and referred to as *the* dielectric permittivity of the material.

Yet, another set of experimental data [10–13] indicates that the dielectric constitutive relation between $\mathbf{d}$ and $\mathbf{e}$ in a dielectric elastomer may in fact strongly *depend* on the deformations the material undergoes. In contrast with the case of ideal dielectrics detailed earlier, these materials have been described as having a "deformation-dependent permittivity." Although intuitively descriptive, this terminology is slightly misleading since, strictly speaking and as recalled above, the dielectric permittivity is *the constant* second-order tensor that relates the electric displacement and the electric field when the material is not deformed and subjected only to small electric fields. To avoid this ambiguity, in this work, these materials will instead be referred to as exhibiting an *apparent* permittivity $\widehat{\boldsymbol{\varepsilon}}_{\mathrm{m}}(\mathbf{F})$ that depends explicitly on the gradient $\mathbf{F}$ of the deformation they undergo. This terminology also makes it clear that the relation between $\mathbf{d}$ and $\mathbf{e}$ remains linear as far as the dielectric variables are concerned, namely,

$$\mathbf{d} = \widehat{\boldsymbol{\varepsilon}}_{\mathrm{m}}(\mathbf{F})\mathbf{e} \tag{2}$$

Aside from dielectric elastomers, dielectric elastomer composites are now being considered as promising pathways to enabling the breadth of technological applications envisioned for stretchable dielectrics due to their superior electromechanical properties [14–21]. These materials are made out of a soft insulating elastomer matrix—in other words, a dielectric elastomer—embedding typically high-permittivity or (semi-)conducting particles. While current frameworks [22–27] for the electromechanical response of dielectric elastomer composites treat the dielectric elastomer matrix as an ideal dielectric, this work is concerned with dielectric elastomer composites composed of a dielectric elastomer matrix with a *deformation-dependent* apparent permittivity of the form

$$\mathbf{d} = [m_{\mathrm{m}}\mathbf{I} + (\varepsilon_{\mathrm{m}} - m_{\mathrm{m}})\mathbf{F}\mathbf{F}^{T}]\mathbf{e} \tag{3}$$

which has recently been shown to accurately capture the deformation-dependent dielectric response of typical dielectric elastomers, see, e.g., Ref. [28] based on the experimental data reported in Ref. [13] for the dielectric elastomer VHB 4910 from 3M. It follows from Eq. (2) and the above discussion that the dielectric constitutive relation (3) is that of a dielectric elastomer with a deformation-dependent apparent permittivity of the form

$$\widehat{\boldsymbol{\varepsilon}}_{\mathrm{m}}(\mathbf{F}) = m_{\mathrm{m}}\mathbf{I} + (\varepsilon_{\mathrm{m}} - m_{\mathrm{m}})\mathbf{F}\mathbf{F}^{T} \tag{4}$$

Contributed by the Applied Mechanics Division of ASME for publication in the Journal of Applied Mechanics. Manuscript received March 31, 2020; final manuscript received May 16, 2020; published online June 4, 2020. Assoc. Editor: Yonggang Huang.

where ε_m and m_m are two material parameters that correspond to the dielectric permittivity and the electrostriction coefficient of the dielectric elastomer matrix.

After recording some preliminary remarks in Sec. 2, a simple explicit formula is proposed in Sec. 3 and shown—via comparison with full-field finite-element (FE) simulations—to accurately describe the elastic dielectric response of isotropic dielectric elastomer composites made out of a neo-Hookean matrix with deformation-dependent apparent permittivity of the form (4), filled with ideal elastic dielectric particles. This result generalizes the simple homogenization formula of Lefèvre and Lopez-Pamies [26] for isotropic dielectric elastomer composites with a neo-Hookean ideal elastic dielectric matrix and is recorded here for convenience.

The elastic dielectric response of an elastic dielectric with (incompressible) free-energy function $W_m = \mu_m[I_1 - 3]/2 + (m_m - \varepsilon_m)I_4^E/2 - m_m I_5^E/2$ *, filled with any type of non-percolative isotropic distribution of ideal elastic dielectric particles with (incompressible) free-energy function* $W_p = \mu_p[I_1 - 3]/2 - \varepsilon_p I_5^E/2$ *is characterized by the (incompressible) free-energy function*

$$W = \frac{\mu}{2}[I_1 - 3] + \frac{m - \varepsilon}{2} I_4^E - \frac{m}{2} I_5^E$$

where $I_1 = \mathbf{F}\cdot\mathbf{F}$, $I_4^E = \mathbf{E}\cdot\mathbf{E}$, *and* $I_5^E = \mathbf{F}^{-T}\mathbf{E}\cdot\mathbf{F}^{-T}\mathbf{E}$ *are isotropic invariants of the deformation gradient* $\mathbf{F}$ *and Lagrangian electric field* $\mathbf{E} = \mathbf{F}^{-T}\mathbf{e}$*, while the coefficients* μ*,* ε*, and* m *stand for the shear modulus, dielectric permittivity, and electrostrictive constant that characterize the response of the composite material in the asymptotic limit of small deformations and moderate electric fields.*

Similarly, a closed-form approximation is put forth in Sec. 4 for the elastic dielectric response of isotropic dielectric elastomer composites made out of a non-Gaussian matrix with deformation-dependent apparent permittivity of the form (4), filled with nonlinear elastic dielectric particles. This result constitutes a generalization of an earlier result by Lefèvre and Lopez-Pamies [27] for isotropic dielectric elastomer composites comprising a non-Gaussian ideal dielectric matrix and is recorded here as well for convenience.

The elastic dielectric response of a non-Gaussian dielectric elastomer with (incompressible) free-energy function $W_m = \psi_m(I_1) + (m_m - \varepsilon_m)/2\, I_4^E - m_m/2\, I_5^E$*, filled with any type of non-percolative isotropic distribution of nonlinear elastic dielectric particles with (incompressible) free-energy function* $W_p = \mu_p/2\,[I_1 - 3] - \mathcal{S}_p(I_5^E)$ *at volume fraction* c*, is characterized by the (incompressible) free-energy function*

$$W = (1-c)\psi_m(\mathcal{I}_1) - \frac{(1-c)z}{2}[\mathcal{I}_1 - 3] + \frac{n(z)}{2}[I_1 - 3] - c\mathcal{S}_p(\mathcal{I}_5) + \frac{c\xi}{2}\mathcal{I}_5 + \frac{\omega(z,\xi) - \nu(\xi)}{2} I_4^E - \frac{\omega(z,\xi)}{2} I_5^E$$

with

$$\mathcal{I}_1 = \frac{1}{1-c}\frac{\partial n}{\partial z}(z)[I_1 - 3] + \frac{1}{1-c}\frac{\partial \omega}{\partial z}(z,\xi)\big[I_4^E - I_5^E\big] + 3$$

$$\mathcal{I}_5 = -\frac{1}{c}\left(\frac{\partial \omega}{\partial \xi}(z,\xi) - \frac{\partial \nu}{\partial \xi}(\xi)\right) I_4^E + \frac{1}{c}\frac{\partial \omega}{\partial \xi}(z,\xi) I_5^E$$

and $n(z)$*,* $\nu(\xi)$*,* $\omega(z,\xi)$ *are microstructure-dependent coefficients that are defined in terms of the solutions of two uncoupled linear pdes (given by expressions (33)), while the variables* z *and* ξ *are implicitly defined as the solution of the following system of two nonlinear algebraic equations:*

$$\mathcal{F}_1\{z,\xi\} = 2\psi_m'(\mathcal{I}_1) - z = 0$$
$$\mathcal{F}_2\{z,\xi\} = 2\mathcal{S}_p'(\mathcal{I}_5) - \xi = 0$$

In order to facilitate the use of the above two general results, their specializations to the practically relevant cases of rigid and liquid-like spherical particles are also recorded in Secs. 3.2 and 4.2, respectively.

Finally, the above results are deployed in Sec. 5 to probe the electrostriction response of dielectric elastomer composites made out of the typical dielectric elastomer VHB 4910 which possesses a deformation-dependent apparent permittivity [13]. It is shown that the elastic dielectric response of the dielectric elastomer composite strongly depends on the deformation-dependent apparent permittivity of the matrix it comprises.

2 Preliminaries

2.1 Kinematics. Consider a homogeneous deformable dielectric solid occupying a domain Ω_0 in its undeformed initial configuration, with material points being identified by their initial position vector $\mathbf{X} \in \Omega_0$. When subjected to external stimuli, the material occupies a different configuration Ω after material points move to new positions identified by $\mathbf{x} = \chi(\mathbf{X})$, with $\chi(\mathbf{X})$ a one-to-one mapping between Ω_0 and Ω. The deformation gradient then corresponds to $\mathbf{F} = \mathrm{Grad}\,\chi$.

2.2 Constitutive Modeling. Following now common practice, the elastic dielectric response of the solid is characterized by a "total" free-energy function [29,30], $W(\mathbf{F}, \mathbf{E})$, taken to be an objective function of the deformation gradient $\mathbf{F}$ and an objective and even function of the Lagrangian electric field $\mathbf{E}$. It follows then that the "total" first Piola–Kirchhoff stress $\mathbf{S}$ and Lagrangian electric displacement $\mathbf{D}$ at any given material point $\mathbf{X} \in \Omega_0$ are given by

$$\mathbf{S}(\mathbf{X}) = \frac{\partial W}{\partial \mathbf{F}}(\mathbf{F}, \mathbf{E}) \quad \text{and} \quad \mathbf{D}(\mathbf{X}) = -\frac{\partial W}{\partial \mathbf{E}}(\mathbf{F}, \mathbf{E}) \tag{5}$$

Remark 1 (F–D formulation). The elastic dielectric response of the solid can be alternatively characterized by a free-energy function $W^*(\mathbf{F}, \mathbf{D})$, where $\mathbf{F}$ and $\mathbf{D}$ are taken as independent variables. It then follows that

$$\mathbf{S}(\mathbf{X}) = \frac{\partial W^*}{\partial \mathbf{F}}(\mathbf{F}, \mathbf{D}) \quad \text{and} \quad \mathbf{E}(\mathbf{X}) = \frac{\partial W^*}{\partial \mathbf{D}}(\mathbf{F}, \mathbf{D}) \tag{6}$$

Moreover, when the free energy $W(\mathbf{F}, \mathbf{E})$ is concave in $\mathbf{E}$, the connection

$$W^*(\mathbf{F}, \mathbf{D}) = \sup_{\mathbf{E}} \{\mathbf{D}\cdot\mathbf{E} + W(\mathbf{F}, \mathbf{E})\} \tag{7}$$

holds between $W(\mathbf{F}, \mathbf{E})$ and $W^*(\mathbf{F}, \mathbf{D})$ while if $W^*(\mathbf{F}, \mathbf{D})$ is convex in $\mathbf{D}$, the relation

$$W(\mathbf{F}, \mathbf{E}) = -\sup_{\mathbf{D}} \{\mathbf{D}\cdot\mathbf{E} - W^*(\mathbf{F}, \mathbf{D})\}$$

holds between them.

Remark 2 (Eulerian quantities). The "total" Cauchy stress $\boldsymbol{\sigma}$, Eulerian electric field $\mathbf{e}$, and Eulerian electric displacement $\mathbf{d}$ are related to their Lagrangian counterparts by the relations

$$\boldsymbol{\sigma} = \frac{1}{\det \mathbf{F}}\mathbf{S}\mathbf{F}^T, \quad \mathbf{e} = \mathbf{F}^{-T}\mathbf{E}, \quad \mathbf{d} = \frac{1}{\det \mathbf{F}}\mathbf{F}\mathbf{D} \tag{8}$$

while the electric polarization $\mathbf{p}$ is given by

$$\mathbf{p} = \mathbf{d} - \varepsilon_0 \mathbf{e} \tag{9}$$

where $\varepsilon_0 \approx 8.85$ pF/m stands for the dielectric permittivity of vacuum.

Remark 3 (Isotropic invariants). For isotropic materials, the main interest of this work, the free energy $W(\mathbf{F}, \mathbf{E})$ can be written down as a function of six standard invariants, $W(\mathbf{F}, \mathbf{E}) = W(I_1, I_2, J, I_4^E, I_5^E, I_6^E)$, with

$$I_1 = \mathrm{tr}\,\mathbf{C}, \quad I_2 = \frac{1}{2}\big[(\mathrm{tr}\,\mathbf{C})^2 - \mathrm{tr}\,\mathbf{C}^2\big], \quad J = \det\mathbf{F} \tag{10}$$

and

$$I_4^E = \mathbf{E}\cdot\mathbf{E},\quad I_5^E = \mathbf{E}\cdot\mathbf{C}^{-1}\mathbf{E},\quad I_6^E = \mathbf{E}\cdot\mathbf{C}^{-2}\mathbf{E} \tag{11}$$

where $\mathbf{C}=\mathbf{F}^T\mathbf{F}$ is the right-Cauchy-Green deformation tensor.

Similarly, the free energy $W^*(\mathbf{F},\mathbf{D})$ can be represented as a function of six standard invariants, the three mechanical invariants (10) and

$$I_4^D = \mathbf{D}\cdot\mathbf{D},\quad I_5^D = \mathbf{D}\cdot\mathbf{C}\mathbf{D},\quad I_6^D = \mathbf{D}\cdot\mathbf{C}^2\mathbf{D}$$

so that $W^*(\mathbf{F},\mathbf{D}) = W^*(I_1, I_2, J, I_4^D, I_5^D, I_6^D)$.

2.3 Non-Gaussian Dielectric Elastomers With Deformation-Dependent Apparent Permittivity. As alluded to in Sec. 1, the focus of this work is on isotropic incompressible dielectric elastomer composites composed of an incompressible non-Gaussian dielectric elastomer with deformation-dependent apparent permittivity of the form (4). To this end, the elastic dielectric response of the dielectric elastomer matrix is taken to be characterized by a free-energy function of the form

$$W_{\rm m}(\mathbf{F},\mathbf{E}) = \begin{cases} \psi_{\rm m}(I_1) + \frac{m_{\rm m}-\varepsilon_{\rm m}}{2} I_4^E - \frac{m_{\rm m}}{2} I_5^E & \text{if } J=1 \\ +\infty & \text{otherwise} \end{cases} \tag{12}$$

where $\varepsilon_{\rm m}$ and $m_{\rm m}$ stand for the permittivity and the electrostriction coefficient of the dielectric elastomer, respectively.[1] With help of relations $(5)_2$, $(8)_{2,3}$, and $(11)_{1,2}$, it is not difficult to show that this choice precisely describes a solid satisfying the dielectric constitutive relation (3) with deformation-dependent apparent permittivity of the form (4). In the above expression, the function $\psi_{\rm m}(I_1)$ is an arbitrary function of choice that describes the elastic response of the dielectric elastomer. Physical considerations entail that $\psi_{\rm m}(I_1)$ satisfies the requirements $\psi_{\rm m}(3)=0$ and $\psi'_{\rm m}(3)=\mu_{\rm m}/2$, with $\mu_{\rm m}>0$ the shear modulus of the dielectric elastomer. Examples for the function $\psi_{\rm m}(I_1)$ include for instance the neo-Hookean [31], Arruda-Boyce [32], Gent [33], and Lopez-Pamies [34] models.

2.4 Nonlinear Elastic Dielectric Particles With Possible Polarization Saturation. Concentrating on nonlinear elastic dielectric particles prompts considering free-energy functions of the form

$$W_{\rm p}(\mathbf{F},\mathbf{E}) = \begin{cases} \frac{\mu_{\rm p}}{2}[I_1-3] - \mathcal{S}_{\rm p}(I_5^E) & \text{if } J=1 \\ +\infty & \text{otherwise} \end{cases} \tag{13}$$

to describe their elastic dielectric response. In this expression, $\mu_{\rm p}$ stands for the shear modulus of the particles and $\mathcal{S}_{\rm p}(I_5^E)$ is a function of choice to characterize their dielectric response. Physical considerations entail that $\mathcal{S}_{\rm p}(I_5^E)$ satisfies the requirements $\mathcal{S}_{\rm p}(0)=0$, $\mathcal{S}'_{\rm p}(0)=\varepsilon_{\rm p}/2$ with $\varepsilon_{\rm p}>0$ the permittivity of the particles, as well as the convexity conditions $\mathcal{S}'_{\rm p}(I_5^E)>0$ and $\mathcal{S}'_{\rm p}(I_5^E)+2I_5^E\mathcal{S}''_{\rm p}(I_5^E)>0$. While the choice $\mathcal{S}_{\rm p}(I_5^E)=\varepsilon_{\rm p}I_5^E/2$ corresponds to ideal dielectric particles, other choices can be used for instance to describe the saturation of the polarization of the particles to a value $p_{\rm p}^s$ at large electric fields. Granted that the polarization of the particles is given by $\mathbf{p}=\left[2\mathcal{S}'_{\rm p}(I_5^E)-\varepsilon_0\right]\mathbf{e}$, $\mathcal{S}_{\rm p}(I_5^E)$ represents polarization saturation to $p_{\rm p}^s$ so long it satisfies the growth condition $\mathcal{S}'_{\rm p}(I_5^E)=\varepsilon_0/2+p_{\rm p}^s/(2\sqrt{I_5^E})+o(1/\sqrt{I_5^E})$ as $I_5^E\to\infty$. Possible choices of functions $\mathcal{S}_{\rm p}(I_5^E)$ that describe polarization saturation include the Langevin and Brillouin models, see, e.g., Ref. [35].

[1] In addition to their inherent physical meaning in the limit of small deformations and moderate electric fields, insight into $\varepsilon_{\rm m}$ and $m_{\rm m}$ can be gained when the dielectric elastomer undergoes a biaxial stretch. Then, the apparent permittivity $\widehat{\varepsilon}_\perp(\lambda)$ normal to the stretch plane transitions from $\varepsilon_{\rm m}$ to $m_{\rm m}$ as the biaxial stretch $\lambda\geq 1$ increases: $\widehat{\varepsilon}_\perp(\lambda)=m_{\rm m}+(\varepsilon_{\rm m}-m_{\rm m})\lambda^{-4}$.

3 The Case of a Neo-Hookean Matrix Filled With Ideal Dielectric Particles

We begin by considering isotropic incompressible dielectric elastomer composites composed of a neo-Hookean matrix with deformation-dependent apparent permittivity, filled with a distribution of ideal dielectric particles. This case corresponds to the simplest prototype of dielectric elastomer composite with deformation-dependent apparent-permittivity matrix and amounts to choosing the functions

$$\psi_{\rm m}(I_1) = \frac{\mu_{\rm m}}{2}[I_1-3] \quad\text{and}\quad \mathcal{S}_{\rm p}(I_5^E) = \frac{\varepsilon_{\rm p}}{2}I_5^E$$

in Eqs. (12) and (13), with $\mu_{\rm m}$ the shear modulus of the matrix and $\varepsilon_{\rm p}$ the permittivity of the particles. A simple closed-form free energy $W(\mathbf{F},\mathbf{E})$ for any such dielectric elastomer composite is recorded in Sec. 3.1. This result applies to any arbitrary isotropic, two-phase, non-percolative particulate microstructure but is specialized to the practically relevant case of rigid or liquid-like spherical particles in Sec. 3.2 where its accuracy is established by direct comparisons with full-field FE simulations.

3.1 Arbitrary Isotropic, Two-Phase, Non-percolative Particulate Microstructure. We propose here that the elastic dielectric response of an elastic dielectric with free-energy function

$$W_{\rm m}(\mathbf{F},\mathbf{E}) = \begin{cases} \frac{\mu_{\rm m}}{2}[I_1-3] + \frac{m_{\rm m}-\varepsilon_{\rm m}}{2} I_4^E - \frac{m_{\rm m}}{2} I_5^E & \text{if } J=1 \\ +\infty & \text{otherwise} \end{cases} \tag{14}$$

filled with *any non-percolative, two-phase, particulate, isotropic* distribution of ideal elastic dielectric particles with free-energy function

$$W_{\rm p}(\mathbf{F},\mathbf{E}) = \begin{cases} \frac{\mu_{\rm p}}{2}[I_1-3] - \frac{\varepsilon_{\rm p}}{2} I_5^E & \text{if } J=1 \\ +\infty & \text{otherwise} \end{cases} \tag{15}$$

is characterized by the free-energy function

$$W(\mathbf{F},\mathbf{E}) = \begin{cases} \frac{\mu}{2}[I_1-3] + \frac{m-\varepsilon}{2} I_4^E - \frac{m}{2} I_5^E & \text{if } J=1 \\ +\infty & \text{otherwise} \end{cases} \tag{16}$$

Here, μ, ε, and m stand for the shear modulus, permittivity, and electrostrictive constant that characterize the response of the composite in the asymptotic limit of small deformations and moderate electric fields, see Remark 5. They are formally given by

$$\begin{aligned} \mu &= \frac{1}{5|\Omega_0|}\int_{\Omega_0} \mu_1(\mathbf{X})\mathcal{K}_{klmn}\Gamma_{mkl,n}\,d\mathbf{X} \\ \varepsilon &= \frac{1}{3|\Omega_0|}\int_{\Omega_0} \varepsilon_1(\mathbf{X})\gamma_{m,m}\,d\mathbf{X} \\ m &= \frac{1}{5|\Omega_0|}\int_{\Omega_0} m_1(\mathbf{X})\mathcal{K}_{ijkl}\Gamma_{rij,s}\mathcal{K}_{rspq}\gamma_{p,k}\gamma_{q,l}\,d\mathbf{X} \end{aligned} \tag{17}$$

where $\mu_1(\mathbf{X}) = \left[1-\theta_{\rm p}(\mathbf{X})\right]\mu_{\rm m} + \theta_{\rm p}(\mathbf{X})\mu_{\rm p}\varepsilon_1(\mathbf{X}) = \left[1-\theta_{\rm p}(\mathbf{X})\right]\varepsilon_{\rm m} + \theta_{\rm p}(\mathbf{X})\varepsilon_{\rm p}$, and $m_1(\mathbf{X}) = \left[1-\theta_{\rm p}(\mathbf{X})\right]m_{\rm m} + \theta_{\rm p}(\mathbf{X})\varepsilon_{\rm p}$ with $\theta_{\rm p}$ denoting the indicator function of the spatial regions occupied collectively by the particles in Ω_0, $\mathcal{K}_{ijkl} = 1/2(\delta_{ik}\delta_{jl}+\delta_{il}\delta_{jk}) - 1/3\delta_{ij}\delta_{kl}$ with δ_{ij} denoting the Kronecker delta, the notation $_{,i}$ represents partial differentiation with respect to the material point coordinate X_i, and the tensor fields $\mathbf{\Gamma}$ and $\boldsymbol{\gamma}$ are implicitly defined as the solutions of two *uncoupled linear* boundary value problems:

$$\begin{cases} \left[\mu_1(\mathbf{X})\mathcal{K}_{ijmn}\Gamma_{mkl,n} + \delta_{ij}q_{kl}\right]_{,j} = 0, & \mathbf{X}\in\Omega_0 \\ \Gamma_{mkl,m} = 0, & \mathbf{X}\in\Omega_0 \\ \Gamma_{ikl} = \delta_{ik}X_l, & \mathbf{X}\in\partial\Omega_0 \end{cases} \tag{18}$$

where $\mathbf{q}(\mathbf{X})$ is a pressure-like second-order tensor associated with the incompressibility constraint $\Gamma_{mkl,m}=0$ in Ω_0 and

$$\begin{cases} \left[\varepsilon_1(\mathbf{X})\gamma_{i,j}\right]_{,i}=0, & \mathbf{X}\in\Omega_0 \\ \gamma_i = X_i, & \mathbf{X}\in\partial\Omega_0 \end{cases} \tag{19}$$

Remark 4 (Meaning of the variables and parameters). It is recalled here that in expressions (14)–(16), I_1, J, I_4^E, and I_5^E stand for isotropic invariants of $\mathbf{F}$ and $\mathbf{E}$ defined by Eqs. $(10)_{1,3}$ and $(11)_{1,2}$, μ_m, ε_m, m_m correspond to the shear modulus, permittivity, and electrostrictive coefficient of the matrix with free energy (14), while μ_p and ε_p correspond to the shear modulus and permittivity of the particles with free energy (15).

Remark 5 (Small deformation limit). By construction, the free energy (16) is exact in the asymptotic limit of small deformations and moderate electric fields, that is, when $\mathbf{H}\doteq\mathbf{F}-\mathbf{I}=O(\zeta)$ and $\mathbf{E}=O(\zeta^{1/2})$ for a vanishingly small parameter ζ [26,36,37]. It reduces asymptotically to

$$W(\mathbf{F},\mathbf{E})=\begin{cases} \mu\mathbf{H}\cdot\mathbf{H}-\frac{\varepsilon}{2}\mathbf{E}\cdot\mathbf{E}+m\mathbf{E}\cdot\mathbf{H}\mathbf{E} & \text{if } \operatorname{tr}\mathbf{H}=0 \\ +\infty & \text{otherwise} \end{cases} \tag{20}$$

and implies the constitutive relations

$$\mathbf{S}=\mu(\mathbf{H}+\mathbf{H}^T)+m\mathbf{E}\otimes\mathbf{E}-q\mathbf{I} \quad \text{and} \quad \mathbf{D}=\varepsilon\mathbf{E} \tag{21}$$

to leading order in ζ with q the hydrostatic pressure associated with the incompressibility constraint $\operatorname{tr}\mathbf{H}=0$. It is then plain from Eqs. (20) and (21) that the coefficients μ, ε, and m correspond to the shear modulus, permittivity, and electrostrictive constant of this class of dielectric elastomer composites and fully characterize their response in this limit.

The computation of these coefficients requires in general knowledge of the third- and first-order tensors $\boldsymbol{\Gamma}$ and $\boldsymbol{\gamma}$ solutions (18) and (19) which may be obtained, though laboriously, by means of commercial FE packages. However, due to the overall isotropy of the composites studied here, the elastic dielectric coefficients μ, ε, and m can be computed by considering only certain components of $\boldsymbol{\Gamma}$ and $\boldsymbol{\gamma}$ which can then be obtained in a straightforward fashion by means of commercial FE packages, see Refs. [26,38]. It is also worth noting that for some microstructures, the tensors $\boldsymbol{\Gamma}$, $\boldsymbol{\gamma}$ and the elastic dielectric coefficients μ, ε, and m can be worked out analytically, see, e.g., Ref. [39] for differential coated sphere assemblages.

Remark 6 (Finite deformations and electric fields). For arbitrary deformations and electric fields, the free energy (16) is only in general an approximation. Its accuracy was however demonstrated in Ref. [26] by direct comparisons with numerical solutions for a number of different classes of isotropic dielectric elastomer composites comprising an ideal dielectric matrix ($m_m=\varepsilon_m$). We report similar comparisons in Sec. 3.2 to establish the accuracy of Eq. (16) for the more general case of a matrix with deformation-dependent apparent permittivity ($m_m\neq\varepsilon_m$).

Now, making use of Eq. (5), the free energy (16) leads to the following constitutive relations for the first Piola–Kirchhoff total stress $\mathbf{S}$ and electric displacement $\mathbf{D}$:

$$\mathbf{S}=\mu\mathbf{F}+m\mathbf{F}^{-T}\mathbf{E}\otimes\mathbf{F}^{-1}\mathbf{F}^{-T}\mathbf{E}-q\mathbf{F}^{-T}$$
$$\mathbf{D}=(\varepsilon-m)\mathbf{E}+m\mathbf{F}^{-1}\mathbf{F}^{-T}\mathbf{E}$$

where q is the hydrostatic pressure associated with the incompressibility constraint $J=1$. Expressions $(8)_{1,3}$ and (9) for the total Cauchy stress $\boldsymbol{\sigma}$, Eulerian electric displacement $\mathbf{d}$, and polarization $\mathbf{p}$ then lead to

$$\boldsymbol{\sigma}=\mu\mathbf{F}\mathbf{F}^T+m\mathbf{e}\otimes\mathbf{e}-q\mathbf{I}, \quad \mathbf{d}=m\mathbf{e}+(\varepsilon-m)\mathbf{F}\mathbf{F}^T\mathbf{e}$$
$$\mathbf{p}=(m-\varepsilon_0)\mathbf{e}+(\varepsilon-m)\mathbf{F}\mathbf{F}^T\mathbf{e} \tag{22}$$

It is plain from expression $(22)_2$ that such dielectric elastomer composites also exhibit a deformation-dependent apparent permittivity $\widehat{\boldsymbol{\varepsilon}}(\mathbf{F})=m\mathbf{I}+(\varepsilon-m)\mathbf{F}\mathbf{F}^T$ that is of the same form (4) as that of the matrix they comprise. This characteristic stems from the inherent heterogeneous nature of these materials and not from the deformation-dependent nature of the apparent permittivity of the matrix, as, in general, $m\neq\varepsilon$ even when the matrix is an ideal dielectric ($m_m=\varepsilon_m$), see Ref. [26].

Remark 7 (Functional form of Eq. (16)). A defining feature of expression (16) is its linearity in the invariants I_1, I_4^E, and I_5^E and its independence of the invariants I_2 and I_6^E. This characteristic is exact in the case of small deformations and moderate electric fields [26] and shown to hold approximately for arbitrary deformations and electric fields in Sec. 3.2. In addition, this feature is leveraged in Sec. 4 within the context of nonlinear comparison medium methods [27,40,41] to obtain a free energy for dielectric elastomer composites with a non-Gaussian matrix filled with particles with possible polarization saturation, that is, arbitrary choices of functions $\psi_m(I_1)$ and $\mathcal{S}_p(I_5^E)$ in Eqs. (12) and (13).

Remark 8 (F–D formulation). The free energy $W^*(\mathbf{F},\mathbf{D})$ corresponding to the free energy $W(\mathbf{F},\mathbf{E})$ given by Eq. (16) can be readily obtained from Eq. (7) and reads

$$W^*(\mathbf{F},\mathbf{D})=\begin{cases} \frac{\mu}{2}[I_1-3]+\dfrac{I_5^D+\eta^2 I_4^D+\eta(I_1I_5^D-I_6^D)}{2m(1+\eta^3+\eta^2I_2+\eta I_1)} & \text{if } J=1 \\ +\infty & \text{otherwise} \end{cases} \tag{23}$$

where $\eta\doteq(\varepsilon-m)/m$. It then follows from Eq. (6) that the first Piola–Kirchhoff stress tensor $\mathbf{S}$ and Lagrangian electric field $\mathbf{E}$ can be written as

$$\mathbf{S}=\mu\mathbf{F}-q\mathbf{F}^{-T}+\frac{1}{m(1+\eta^3+\eta^2I_2+\eta I_1)}\times\left[\eta(I_5^D\mathbf{F}-\mathbf{F}\mathbf{D}\otimes\mathbf{F}^T\mathbf{F}\mathbf{D}-\mathbf{F}\mathbf{F}^T\mathbf{F}\mathbf{D}\otimes\mathbf{D})+(1+\eta I_1)\mathbf{F}\mathbf{D}\otimes\mathbf{D}\right]-\frac{\eta I_5^D+\eta^3I_4^D+\eta^2(I_1I_5^D-I_6^D)}{m(1+\eta^3+\eta^2I_2+\eta I_1)^2}\left[\mathbf{F}-\eta\mathbf{F}^{-T}\mathbf{F}^{-1}\mathbf{F}^{-T}\right]$$

and

$$\mathbf{E}=\frac{1}{m(1+\eta^3+\eta^2I_2+\eta I_1)}\times\left[(1+\eta I_1)\mathbf{F}^T\mathbf{F}\mathbf{D}+\eta^2\mathbf{D}-\eta\mathbf{F}^T\mathbf{F}\mathbf{F}^T\mathbf{F}\mathbf{D}\right]$$

in terms of the deformation gradient $\mathbf{F}$ and the Lagrangian electric displacement $\mathbf{D}$.

Remark 9 (Special case of interest). As already mentioned in Sec. 1, expression (16) reduces to the result by Lefèvre and Lopez-Pamies [26] when the matrix is an ideal dielectric ($m_m=\varepsilon_m$). While the free energy (16) shares its functional form with the result—Eq. (32)—in Ref. [26] it generalizes, the two results differ from the value taken by the electrostrictive coefficient m, which depends explicitly on whether the apparent permittivity of the matrix is deformation-dependent ($m_m\neq\varepsilon_m$) or not ($m_m=\varepsilon_m$).

3.2 Isotropic Distribution of Spherical Particles.

We report next the specialization of the above result to the practical cases of dielectric elastomer composites comprising isotropic distributions of rigid- or liquid-like spherical particles.

3.2.1 Rigid Spherical Particles. The majority of experimental investigations conducted to date on dielectric elastomer composites involve equiaxed filler particles with a shear modulus that is several orders of magnitude higher than that of the dielectric elastomer matrix [14–18,20]. This prompts spelling out the result above in the limit of rigid particles, that is, when $\mu_p=\infty$. In this case, and when the particles are spherical in shape, the elastic dielectric coefficients μ, ε, and m defined by Eq. (17) can be accurately

approximated by

$$\mu = (1-c)^{-5/2}\mu_{\rm m}, \quad \varepsilon = \varepsilon_{\rm m} + \frac{3c(\varepsilon_{\rm p}-\varepsilon_{\rm m})\varepsilon_{\rm m}}{(2+c)\varepsilon_{\rm m}+(1-c)\varepsilon_{\rm p}}$$

$$m = m_{\rm m} + \frac{3c(10+2c+3c^2)(\varepsilon_{\rm p}-\varepsilon_{\rm m})\varepsilon_{\rm m} m_{\rm m}}{5[(2+c)\varepsilon_{\rm m}+(1-c)\varepsilon_{\rm p}]^2} + \frac{3c(1-c)(5+3c)(\varepsilon_{\rm p}-\varepsilon_{\rm m})\varepsilon_{\rm p} m_{\rm m}}{5[(2+c)\varepsilon_{\rm m}+(1-c)\varepsilon_{\rm p}]^2} \tag{24}$$

within the range $c \in [0, 0.25]$ of volume fractions of particles, and for all values of material coefficients $\mu_{\rm m}$, $\varepsilon_{\rm m}$, $m_{\rm m}$, and $\varepsilon_{\rm p}$ of the matrix and particles. The finite branch of the incompressible free energy of isotropic dielectric elastomers composites composed of a neo-Hookean deformation-dependent apparent-permittivity matrix—with free energy (14)—filled with rigid ideal dielectric spherical particles is then given explicitly by

$$W^{r,\rm sph} = \frac{\mu_{\rm m}}{2(1-c)^{5/2}}[I_1 - 3] + \frac{m-\varepsilon}{2} I_4^E - \frac{m}{2} I_5^E \tag{25}$$

with $\mu_{\rm m}$ the shear modulus of the matrix and ε and m given explicitly by Eq. $(24)_{2,3}$. The accuracy of the free energy $W^{r,\rm sph}$ above is established next.

We begin with the asymptotic limit of small deformations and moderate electric fields where, granted Eqs. (20) and (21), it suffices to probe the accuracy of expressions (24) for the elastic dielectric coefficients μ, ε, and m. Given that expressions $(24)_{1,2}$ have already been shown [26,41] to be accurate approximations for μ and ε in the case of rigid spherical particles and that they do not depend on the electrostrictive coefficient of the matrix $m_{\rm m}$, we only focus here on expression $(24)_3$ for the electrostrictive coefficient m. This expression is plotted—normalized by $m_{\rm m}$—in Fig. 1(*a*) (labeled as "Rig. Sph. Analytical") as a function of c and $\varepsilon_{\rm p}$ for the choice $m_{\rm m}/\varepsilon_{\rm m} = 0.6$ which is a representative of the elastic dielectric response of a typical dielectric elastomer with deformation-dependent apparent permittivity [28]. The solid circles in Fig. 1(*a*) (labeled as "Rig. Sph. FE") correspond to FE results for composites made out of a dielectric elastomer with free energy (14) isotropically filled with rigid spherical particles with free energy (15) that are monodisperse in size, see Remark 5 and Refs. [26,38] for details about these simulations. It is plain from Fig. 1(*a*) that Eq. $(24)_3$ provides an accurate representation of the electrostrictive coefficient m.

Next, we probe the accuracy of the proposed free energy (25) with Eq. $(24)_{2,3}$ for arbitrary deformations and arbitrary electric fields as well as investigate its particular functional form, that is, its linearity in the invariants I_1, I_4^E, and I_5^E and its independence of I_2 and I_6^E, see Remark 7. This is achieved by direct comparisons with full-field FE simulations for a dielectric elastomer with free energy (14) and $m_{\rm m}/\varepsilon_{\rm m} = 0.6$ isotropically filled with a volume fraction $c = 0.05$ of rigid monodisperse spherical particles with free energy (15) and $\varepsilon_{\rm p}/\varepsilon_{\rm m} = 10^2$; see Refs. [26,27] for details about these simulations. To this end, as shown in Figs. 1(*b*)–1(*f*), the response of the composite is probed along different electromechanical paths for which the value of only one of the invariants I_1,

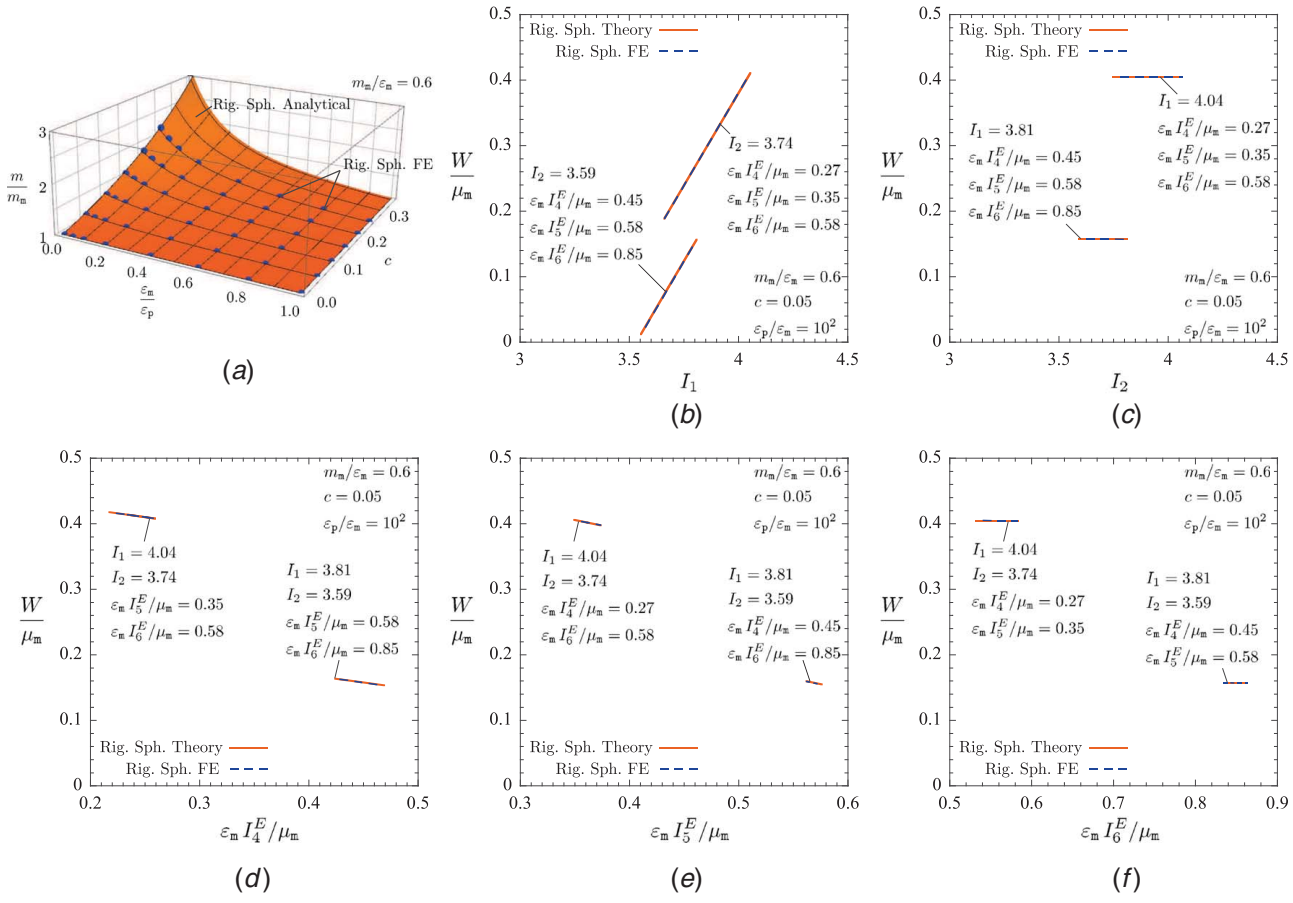

Fig. 1 **(*a*) Plot of the electrostrictive coefficient m—normalized by $m_{\rm m}$—as a function of c and the inverse of the permittivity of the particles $\varepsilon_{\rm p}$—normalized by $\varepsilon_{\rm m}$—for the case of spherical rigid particles when $m_{\rm m}/\varepsilon_{\rm m} = 0.6$. The solid circles ("Rig. Sph. FE") correspond to FE results while the solid surface ("Rig. Sph. Analytical") corresponds to the explicit formula (24). (*b*)–(*f*) Plots of the free energy W for a neo-Hookean deformation-dependent apparent-permittivity matrix filled with a volume fraction $c = 0.05$ of rigid ideal dielectric spherical particles with $m_{\rm m}/\varepsilon_{\rm m} = 0.6$ and $\varepsilon_{\rm p}/\varepsilon_{\rm m} = 10^2$. The solid lines ("Rig. Sph. Theory") correspond to expression (25) with $(24)_{2,3}$ while the dashed lines ("Rig. Sph. FE") correspond to full-field FE simulations.**

I_2, I_4^E, I_5^E, and I_6^E varies, while the other four remain constant in value. The results shown in Figs. 1(*b*)–1(*f*) correspond to two sets of fixed values of the five invariants, $I_1 = 3.81$, $I_2 = 3.59$, $\varepsilon_m I_4^E/\mu_m = 0.45$, $\varepsilon_m I_5^E/\mu_m = 0.58$, $\varepsilon_m I_6^E/\mu_m = 0.85$, and $I_1 = 4.04$, $I_2 = 3.74$, $\varepsilon_m I_4^E/\mu_m = 0.27$, $\varepsilon_m I_5^E/\mu_m = 0.35$, $\varepsilon_m I_6^E/\mu_m = 0.58$. Note that fixing the value of four out of the five invariants imposes bounds on the range of values that the varied invariant can take and that the varied invariant covers the entire range of values it can take; for instance, $3.55 \le I_1 \le 3.81$ for the first set of fixed values and $3.66 \le I_1 \le 4.05$ for the second set of fixed values.

In addition to the results shown in Fig. 1, a large set of comparisons, not reported here for conciseness, has confirmed that expression $(24)_3$ for the electrostrictive coefficient m and the free energy (25) with Eq. $(24)_{2,3}$ remain in good agreement with FE results independently of the ratios m_m/ε_m and $\varepsilon_p/\varepsilon_m$. Expression (25) with Eq. $(24)_{2,3}$ therefore provides an accurate free energy for isotropic dielectric elastomer composites composed of a neo-Hookean deformation-dependent apparent-permittivity matrix with free energy (14) filled with rigid ideal dielectric spherical particles.

3.2.2 Liquid-like Spherical Particles. Recent theoretical [22,26,27,28] and experimental [21,42] evidence have suggested that embedding liquid-like particles in dielectric elastomers may significantly enhance their electrostrictive properties. Modeling these particles has being incompressible with vanishingly small shear resistance then prompts taking the limit $\mu_p = 0$ in the results presented in Sec. 3.1. In this case, and when the filler particles are spherical in shape in their undeformed configuration, the expressions

$$\mu = (1-c)^{5/3}\mu_m, \quad \varepsilon = \varepsilon_m + \frac{3c(\varepsilon_p - \varepsilon_m)\varepsilon_m}{(2+c)\varepsilon_m + (1-c)\varepsilon_p}$$
$$m = m_m + \frac{c^2\left(400 - 729c^{11/25}\right)(\varepsilon_p - \varepsilon_m)^2\varepsilon_m}{500[(2+c)\varepsilon_m + (1-c)\varepsilon_p]^2}$$
$$+ \frac{3c\varepsilon_m(5\varepsilon_m\varepsilon_p - 3\varepsilon_m m_m - 2\varepsilon_p m_m)}{[(2+c)\varepsilon_m + (1-c)\varepsilon_p]^2} \tag{26}$$

are accurate approximations of the elastic dielectric coefficients μ, ε, and m—defined by Eq. (17)—within the range $c \in [0, 0.25]$ of volume fractions of particles, and for all values of material parameters μ_m, ε_m, m_m, ε_p. As demonstrated next, the finite branch of the incompressible free energy of isotropic dielectric elastomers composites composed of a neo-Hookean deformation-dependent apparent-permittivity matrix with free energy (14) filled with liquid-like ideal dielectric spherical particles can then be accurately represented by

$$W^{l,\mathrm{sph}} = \frac{\mu_m}{2}(1-c)^{5/3}[I_1 - 3] + \frac{m-\varepsilon}{2} I_4^E - \frac{m}{2} I_5^E \tag{27}$$

with μ_m the shear modulus of the matrix and ε and m given explicitly by Eq. $(26)_{2,3}$.

In the same fashion as above for the case of rigid spherical particles, expression $(26)_3$ is plotted—normalized by m_m—in Fig. 2(*a*) (labeled as "Liq. Sph. Analytical") as a function of c

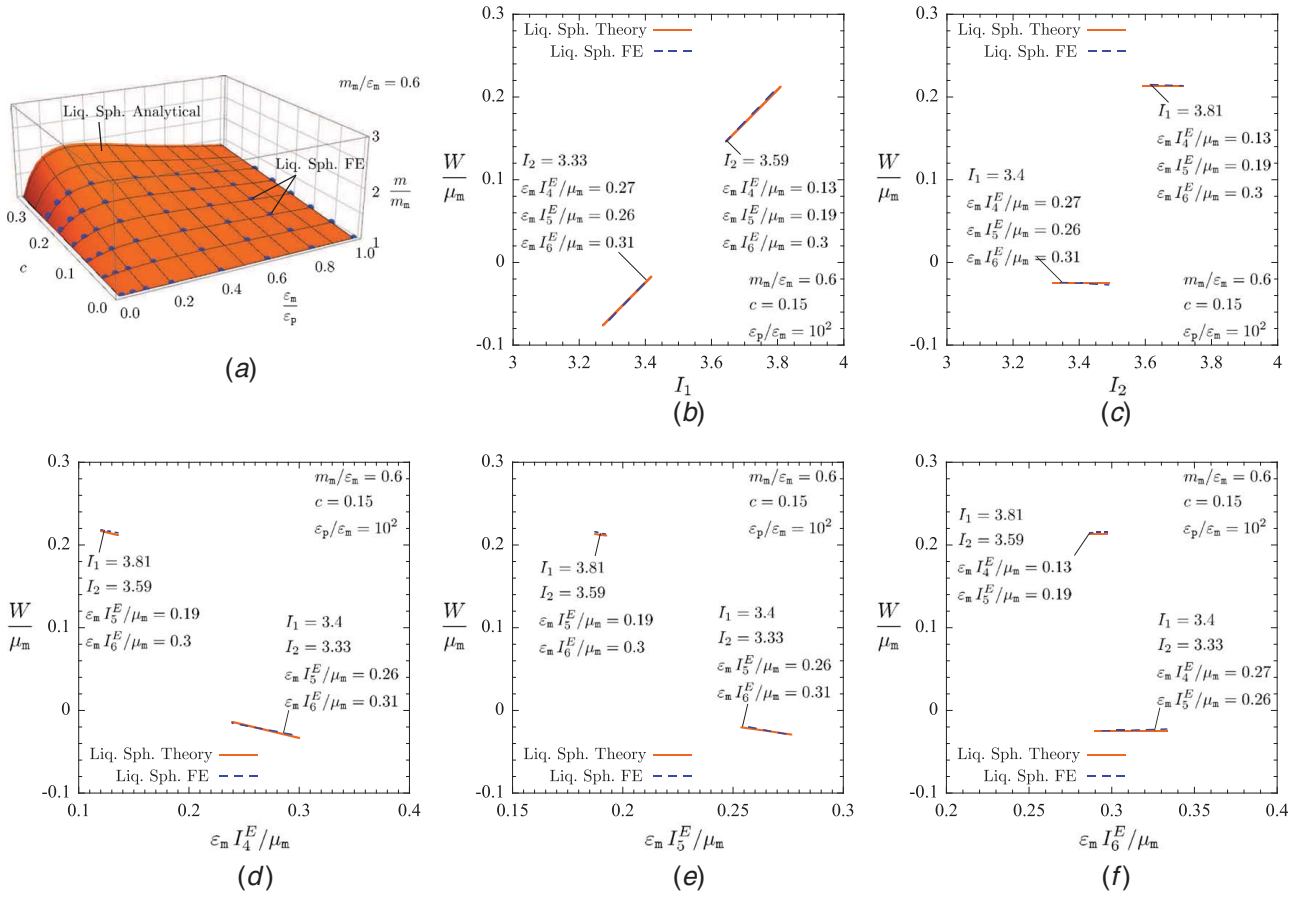

Fig. 2 (*a*) Plot of the electrostrictive coefficient m—normalized by m_m—as a function of c and the inverse of the permittivity of the particles ε_p—normalized by ε_m—for the case of spherical liquid-like particles when $m_m/\varepsilon_m = 0.6$. The solid circles ("Liq. Sph. FE") correspond to FE results while the solid surface ("Liq. Sph. Analytical") corresponds to the explicit formula (26). (*b*)–(*f*) Plots of the free energy W for a neo-Hookean deformation-dependent apparent-permittivity matrix filled with a volume fraction $c = 0.05$ of liquid-like ideal dielectric spherical particles with $m_m/\varepsilon_m = 0.6$ and $\varepsilon_p/\varepsilon_m = 10^2$. The solid lines ("Liq. Sph. Theory") correspond to expression (27) with $(26)_{2,3}$ while the dashed lines ("Liq. Sph. FE") correspond to full-field FE simulations.

and ε_p for the choice $m_m/\varepsilon_m = 0.6$. The solid circles in Fig. 2(*a*) (labeled as "Liq. Sph. FE") correspond to FE results for composites made out of a dielectric elastomer with free energy (14) isotropically filled with liquid-like spherical particles with free energy (15) that are monodisperse in size, see Remark 5 and Refs. [26,38] for details about these simulations. Recall that within the asymptotic limit of small deformations and moderate electric fields, it suffices to probe the accuracy of expressions (26) for the elastic dielectric coefficients μ, ε, and m. Note as well that expressions $(26)_{1,2}$ have already been shown [26] to be accurate approximations for μ and ε in the case of liquid-like spherical particles and that they do not depend on the electrostrictive coefficient of the matrix m_m.

Similar to Figs. 1(*b*)–1(*f*) for rigid spherical particles, the free energy (27) with $(26)_{2,3}$ is plotted in Figs. 2(*b*)–2(*f*) for specific electromechanical loadings that correspond to fixing the value of four out of the five invariants I_1, I_2, I_4^E, I_5^E, and I_6^E while the remaining invariant varies. Corresponding results from full-field FE simulations are also plotted in Figs. 2(*b*)–2(*f*) for a dielectric elastomer with free energy (14) and $m_m/\varepsilon_m = 0.6$ isotropically filled with a volume fraction $c = 0.15$ of liquid-like monodisperse spherical particles with free energy (15) and $\varepsilon_p/\varepsilon_m = 10^2$, see Refs. [26,27] for details about these simulations. The good agreement between the two sets of results demonstrates the accuracy of the proposed free energy (27) with $(26)_{2,3}$ for the case of liquid-like spherical particles and supports that it is approximately linear in the invariants I_1, I_4^E, and I_5^E and independent of I_2 and I_6^E, see Remark 7.

A large set of results has confirmed that expression $(26)_3$ for the electrostrictive coefficient m and free energy (27) with $(26)_{2,3}$ remain in good agreement with corresponding FE results independently of the ratios m_m/ε_m and $\varepsilon_p/\varepsilon_m$. This supports that expression (27) with $(26)_{2,3}$ is an accurate free energy for the elastic dielectric response of neo-Hookean deformation-dependent apparent-permittivity elastomers with free energy (14) isotropically filled with liquid-like ideal dielectric spherical particles.

4 The Case of a Non-Gaussian Matrix Filled With Nonlinear Elastic Dielectric Particles

We put forth in this section a free energy for the elastic dielectric response of non-Gaussian dielectric elastomers with deformation-dependent apparent permittivity that are isotropically filled with nonlinear elastic dielectric particles. This corresponds to any appropriate choices of functions $\psi_m(I_1)$ and $\mathcal{S}_p(I_5^E)$ in Eqs. (12) and (13) to describe the elasticity of the matrix and the polarization of the particles. The proposed free energy is obtained by means of a nonlinear comparison medium method [27,40,41] in nonlinear electrostatics and leverages the free energy (16) for neo-Hookean dielectric elastomers embedding ideal elastic dielectric particles derived in Sec. 3. The general formulation of the proposed result is recorded in Sec. 4.1 and applies to arbitrary isotropic, two-phase, non-percolative particulate microstructures while its specialization to the practically relevant cases of rigid or liquid-like spherical particles is laid out in Sec. 4.2. Here again, the accuracy of the proposed free energy is established by direct comparisons with full-field FE simulations.

4.1 Arbitrary Isotropic, Two-Phase, Non-percolative Particulate Microstructure.

The elastic dielectric response of an elastic dielectric with free energy

$$W_m(\mathbf{F},\mathbf{E}) = \begin{cases} \psi_m(I_1) + \frac{m_m - \varepsilon_m}{2} I_4^E - \frac{m_m}{2} I_5^E & \text{if } J = 1 \\ +\infty & \text{otherwise} \end{cases} \tag{28}$$

filled with *any type of non-percolative, two-phase, particulate, isotropic* distribution of elastic dielectric particles with free energy

$$W_p(\mathbf{F},\mathbf{E}) = \begin{cases} \frac{\mu_p}{2}[I_1 - 3] - \mathcal{S}_p(I_5^E) & \text{if } J = 1 \\ +\infty & \text{otherwise} \end{cases} \tag{29}$$

is characterized by the free energy

$$W(\mathbf{F},\mathbf{E}) = \begin{cases} (1-c)\psi_m(\mathcal{I}_1) - \frac{(1-c)z}{2}[\mathcal{I}_1 - 3] \\ +\frac{n(z)}{2}[I_1 - 3] - c\mathcal{S}_p(\mathcal{I}_5) + \frac{c\xi}{2}\mathcal{I}_5 & \text{if } J = 1 \\ +\frac{\omega(z,\xi)-\nu(\xi)}{2} I_4^E - \frac{\omega(z,\xi)}{2} I_5^E \\ +\infty & \text{otherwise} \end{cases} \tag{30}$$

with

$$\begin{aligned} \mathcal{I}_1 &= \frac{1}{1-c}\frac{\partial n}{\partial z}(z)[I_1 - 3] + \frac{1}{1-c}\frac{\partial \omega}{\partial z}(z,\xi)\left[I_4^E - I_5^E\right] + 3 \\ \mathcal{I}_5 &= -\frac{1}{c}\left(\frac{\partial \omega}{\partial \xi}(z,\xi) - \frac{\partial \nu}{\partial \xi}(\xi)\right) I_4^E + \frac{1}{c}\frac{\partial \omega}{\partial \xi}(z,\xi) I_5^E \end{aligned} \tag{31}$$

where the variables z and ξ are implicitly defined as the solutions of the system of two nonlinear algebraic equations

$$\begin{aligned} \mathcal{F}_1\{z,\xi\} &\doteq 2\psi_m'(\mathcal{I}_1) - z = 0 \\ \mathcal{F}_2\{z,\xi\} &\doteq 2\mathcal{S}_p'(\mathcal{I}_5) - \xi = 0 \end{aligned} \tag{32}$$

In the above expressions, $n(z)$, $\nu(\xi)$, and $\omega(z,\xi)$ are given by

$$\begin{aligned} n(z) &= \frac{1}{5|\Omega_0|}\int_{\Omega_0} \mu_{l,c}(\mathbf{X})\mathcal{K}_{klmn}\Gamma_{mkl,n}\mathrm{d}\mathbf{X} \\ \nu(\xi) &= \frac{1}{3|\Omega_0|}\int_{\Omega_0} \varepsilon_{l,c}(\mathbf{X})\gamma_{m,m}\mathrm{d}\mathbf{X} \\ \omega(z,\xi) &= \frac{1}{5|\Omega_0|}\int_{\Omega_0} m_{l,c}(\mathbf{X})\mathcal{K}_{ijkl}\Gamma_{rij,s}\mathcal{K}_{rspq}\gamma_{p,k}\gamma_{q,l}\mathrm{d}\mathbf{X} \end{aligned} \tag{33}$$

where $\mu_{l,c}(\mathbf{X}) = \left[1 - \theta_p(\mathbf{X})\right]z + \theta_p(\mathbf{X})\mu_p$, $\varepsilon_{l,c}(\mathbf{X}) = \left[1 - \theta_p(\mathbf{X})\right]\varepsilon_m + \theta_p(\mathbf{X})\xi$, $m_{l,c}(\mathbf{X}) = \left[1 - \theta_p(\mathbf{X})\right]m_m + \theta_p(\mathbf{X})\varepsilon_p$ and the tensor fields $\boldsymbol{\Gamma}$ and $\boldsymbol{\gamma}$ are defined as the solutions of the two uncoupled linear boundary value problems

$$\begin{cases} \left[\mu_{l,c}(\mathbf{X})\mathcal{K}_{ijmn}\Gamma_{mkl,n} + \delta_{ij}q_{kl}\right]_{,j} = 0, & \mathbf{X} \in \Omega_0 \\ \Gamma_{mkl,m} = 0, & \mathbf{X} \in \Omega_0 \\ \Gamma_{ikl} = \delta_{ik}X_l, & \mathbf{X} \in \partial\Omega_0 \end{cases} \tag{34}$$

where $\mathbf{q}(\mathbf{X})$ is a pressure-like second-order tensor associated with the incompressibility constraint $\Gamma_{mkl,m} = 0$ in Ω_0 and

$$\begin{cases} \left[\varepsilon_{l,c}(\mathbf{X})\gamma_{i,j}\right]_{,i} = 0, & \mathbf{X} \in \Omega_0 \\ \gamma_i = X_i, & \mathbf{X} \in \partial\Omega_0 \end{cases} \tag{35}$$

Remark 10 (Meaning of the variables and parameters). We begin by recalling here that in the above expressions, I_1, J, I_4^E, and I_5^E stand for isotropic invariants of $\mathbf{F}$ and $\mathbf{E}$ defined by Eqs. $(10)_{1,3}$ and $(11)_{1,2}$, $\psi_m(\mathcal{I}_1)$ is a function of choice that describes the elasticity of the dielectric elastomer matrix while ε_m and m_m correspond to its permittivity and electrostrictive coefficient, and μ_p corresponds to the shear modulus the particles while $\mathcal{S}_p'(\mathcal{I}_5)$ describe the specifics of their polarization.

Now, as above-mentioned, the free energy (30) was obtained by way of a nonlinear comparison medium method. We do not provide the derivation here as it closely follow the one in Ref. [27] but detail nonetheless its key steps. Comparison medium methods are analytical techniques that allow for the derivation of variational solutions for the free energy of the composite of interest based on the response of another material, the so-called comparison medium, see Fig. 3 for a schematic. Here, the comparison medium is chosen to be itself a dielectric elastomer composite, and more specifically, to be of the type studied in Sec. 3. It is made out of a matrix with incompressible free energy $W_{m,c} = z[I_1 - 3]/2 + (m_m - \varepsilon_m)I_4^E/2 - m_m I_5^E/2$, filled with the same isotropic distribution of particles—with incompressible free energy $W_{p,c} = \mu_p[I_1 - 3]/2 - \xi I_5^E/2$—as in the composite of interest. It is plain from this choice of comparison medium that

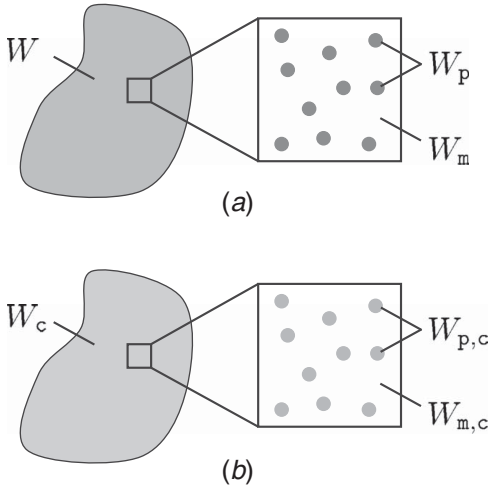

Fig. 3 Schematics of (*a*) the dielectric elastomer composite of interest and (*b*) the choice of nonlinear composite comparison medium

the variable z corresponds physically to the shear modulus of the matrix in the nonlinear composite comparison medium while the variable ξ corresponds physically to the permittivity of the particles in the comparison medium. It then follows from the results in Sec. 3.1 that the elastic dielectric response of this choice of comparison medium is given by the incompressible free energy $W_c = n(z)[\,I_1 - 3]/2 + [\omega(z,\,\xi) - \nu(\xi)]\,I_4^E/2 - \omega(z,\,\xi)\,I_5^E/2$ where the coefficients $n(z)$, $\nu(\xi)$, and $\omega(z,\,\xi)$ correspond physically to the shear modulus, permittivity, and electrostrictive coefficient of the nonlinear composite comparison medium, and following from Eq. (17) are precisely defined by Eq. (33). From there, and making critical use of the Legendre transform $W_c^*(\mathbf{F},\,\mathbf{D}) = \sup_{\mathbf{E}}\{\mathbf{D}\cdot\mathbf{E} + W_c(\mathbf{F},\,\mathbf{E})\}$ that is analogous in form to Eq. (23), the comparison medium framework finally leads to the free energy W given by Eq. (30)—where W_c can be identified—with Eqs. (31)–(32) for the dielectric elastomer composite of interest. We note here that $\mathcal{I}_1$ and $\mathcal{I}_5$ defined by Eq. (31) correspond to "amplified" measure of strains and electric fields at which ψ_m and $\mathcal{S}_p$ are evaluated in Eq. (30) and that the choice of nonlinear composite comparison medium has been "optimized" by taking the shear modulus of its matrix z and permittivity of its particles ξ to be given by as solutions of the two optimality conditions (32) in the form of two nonlinear algebraic equations.

Remark 11 (Small deformation limit). In the limit of small deformations and moderate electric fields, that is again, when $\mathbf{H} = \mathbf{F} - \mathbf{I} = O(\zeta)$ and $\mathbf{E} = O(\zeta^{1/2})$ for a vanishingly small parameter ζ, $\mathcal{I}_1 = 3 + O(\zeta)$ and $\mathcal{I}_5 = O(\zeta)$ so that the nonlinear algebraic equations (32) admit as solutions $z = \mu_m + O(\zeta)$ and $\xi = \varepsilon_p + O(\zeta)$; recall that the functions $\psi_m(I_1)$ and $\mathcal{S}_p(I_5^E)$ must be chosen so that $\psi_m'(3) = \mu_m/2$ and $\mathcal{S}_p'(0) = \varepsilon_p/2$. It follows that the coefficients $n(z)$, $\nu(\xi)$, and $\omega(z,\,\xi)$ defined by Eq. (33) reduce to the elastic dielectric coefficients μ, ε, and m defined by Eq. (17) and the free energy (30) reduces asymptotically to Eq. (20) as expected. The free energy (30) is then by construction asymptotically exact in the limit of small deformations and moderate electric fields.

Remark 12 (Finite deformations and electric fields). For arbitrary deformations and electric fields, the free energy (30) is only a variational approximation. Its accuracy was however demonstrated in Ref. [27] by direct comparisons with numerical solutions for a number of different classes of isotropic dielectric elastomer composites comprising an ideal dielectric matrix ($m_m = \varepsilon_m$). We report similar comparisons in Sec. 4.2 to establish the accuracy of Eq. (30) for the more general case of a matrix with deformation-dependent apparent permittivity ($m_m \neq \varepsilon_m$).

Now, making use of Eq. (5) with the relations $\partial W/\partial\mathcal{I}_1 = \partial W/\partial\mathcal{I}_5 = \partial W/\partial n = \partial W/\partial\nu = 0$ that follow from Eqs. (31) and (32), the free energy (30) leads to the constitutive relations

$$\begin{aligned}\mathbf{S} &= n(z)\mathbf{F} + \omega(z,\,\xi)\mathbf{F}^{-T}\mathbf{E}\otimes\mathbf{F}^{-1}\mathbf{F}^{-T}\mathbf{E} - q\mathbf{F}^{-T}\\ \mathbf{D} &= [\nu(\xi) - \omega(z,\,\xi)]\mathbf{E} + \omega(z,\,\xi)\mathbf{F}^{-1}\mathbf{F}^{-T}\mathbf{E}\end{aligned} \tag{36}$$

where q is the hydrostatic pressure associated with the incompressibility constraint $J = 1$, for the first Piola–Kirchhoff stress $\mathbf{S}$ and electric displacement $\mathbf{D}$. Expressions $(8)_{1,3}$ and (9) for the total Cauchy stress $\boldsymbol{\sigma}$, Eulerian electric displacement $\mathbf{d}$, and polarization $\mathbf{p}$ then lead to

$$\begin{aligned}\boldsymbol{\sigma} &= n(z)\mathbf{F}\mathbf{F}^T + \omega(z,\,\xi)\mathbf{e}\otimes\mathbf{e} - q\mathbf{I}\\ \mathbf{d} &= \omega(z,\,\xi)\mathbf{e} + [\nu(\xi) - \omega(z,\,\xi)]\mathbf{F}\mathbf{F}^T\mathbf{e}\\ \mathbf{p} &= [\omega(z,\,\xi) - \varepsilon_0]\mathbf{e} + [\nu(\xi) - \omega(z,\,\xi)]\mathbf{F}\mathbf{F}^T\mathbf{e}\end{aligned} \tag{37}$$

It is plain from expression $(37)_2$ that such dielectric elastomer composites also exhibit an apparent permittivity $\widehat{\boldsymbol{\varepsilon}}(\mathbf{F},\,\mathbf{E}) = \omega(z,\,\xi)\mathbf{I} + [\nu(\xi) - \omega(z,\,\xi)]\mathbf{F}\mathbf{F}^T$ that depends both on mechanical deformations they undergo and the electric fields they are subjected to; recall that z and ξ—and therefore the precise dependence on deformations and electric fields of this apparent permittivity—depend in general on $\mathbf{F}$ and $\mathbf{E}$ and on the choice of functions $\psi_m(I_1)$ and $\mathcal{S}_p(I_5^E)$ in Eqs. (28) and (29) through Eqs. (31) and (32).

Remark 13 (Functional form of Eq. (30)). A defining feature of the free energy (30) is its independence of the invariants I_2 and I_6^E, which can be traced back to the independence of Eqs. (28) and (29), and—through W_c—(16) of these invariants. As above, this feature is exact in the limit of small deformations and moderate electric fields and is shown in Sec. 4.2 to hold fairly accurately for arbitrary deformations and electric fields.

Remark 14 (F–D formulation). The free energy $W^*(\mathbf{F},\,\mathbf{D})$ corresponding to the free energy $W(\mathbf{F},\,\mathbf{E})$ given by Eq. (30) can be readily obtained from Eq. (7) and reads

$$W^*(\mathbf{F},\,\mathbf{D}) = \begin{cases}(1-c)\psi_m(\mathcal{J}_1) - \frac{z(1-c)}{2}[\mathcal{J}_1 - 3]\\ +\frac{n(z)}{2}[\,I_1 - 3] + c\,\mathcal{S}_p^*(\mathcal{J}_5) - \frac{c}{2\xi}\mathcal{J}_5 + \qquad \text{if } J = 1\\ \dfrac{I_5^D + \rho^2 I_4^D + \rho[I_1 I_5^D - I_6^D]}{2\omega(z,\,\xi)[1 + \rho^3 + \rho^2 I_2 + \rho I_1]}\\ +\infty \qquad\qquad\qquad\qquad\qquad\qquad \text{otherwise}\end{cases}$$

with

$$\begin{aligned}\mathcal{J}_1 = \frac{1}{1-c}\Bigg[&(I_1 - 3)\frac{\partial n}{\partial z}(z) - \frac{1}{\omega(z,\,\xi)^2}\frac{\partial\omega}{\partial z}(z,\,\xi)\\ &\times\Bigg(\frac{3I_4^D\rho^2 + 2\rho[I_1 I_5^D + I_4^D - I_6^D] + [I_1 + 1]I_5^D - I_6^D}{1 + \rho^3 + \rho^2 I_2 + \rho I_1}\\ &- \frac{I_1 + \rho[I_1 + 2I_2] + \rho^2[2I_2 + 3] + 3\rho^3}{[1 + \rho^3 + \rho^2 I_2 + \rho I_1]^2}\\ &\times\left(I_5^D + \rho^2 I_4^D + \rho[I_1 I_5^D - I_6^D]\right)\Bigg)\Bigg] + 3\end{aligned}$$

and

$$\begin{aligned}\mathcal{J}_5 = &\frac{\xi^2}{c\,\omega(z,\,\xi)^2}\frac{\partial\omega}{\partial\xi}(z,\,\xi)\left[\frac{I_5^D + I_4^D\rho^2 + \rho[I_1 I_5^D - I_6^D]}{1 + \rho^3 + \rho^2 I_2 + \rho I_1}\right]\\ &- \frac{\xi^2}{c\,\omega(z,\,\xi)^2}\left[(1+\rho)\frac{\partial\omega}{\partial\xi}(z,\,\xi) - \frac{\partial\nu}{\partial\xi}(\xi)\right]\\ &\times\left[\frac{\left(I_5^D + \rho^2 I_4^D + \rho[I_1 I_5^D - I_6^D]\right)\left(I_1 + 2\rho I_2 + 3\rho^2\right)}{[1 + \rho^3 + \rho^2 I_2 + \rho I_1]^2}\right.\\ &\left.- \frac{I_1 I_5^D - I_6^D + 2\rho I_4^D}{1 + \rho^3 + \rho^2 I_2 + \rho I_1}\right],\end{aligned}$$

with $\rho \doteq (\nu(\xi) - \omega(z,\,\xi))/\omega(z,\,\xi)$ and where the variables z and ξ are defined implicitly as the solutions of the system of two nonlinear

algebraic equations

$$\mathcal{F}_1^*\{z,\xi\} \doteq \psi_{\rm m}'(\mathcal{J}_1) - \frac{z}{2} = 0$$

$$\mathcal{F}_2^*\{z,\xi\} \doteq \mathcal{S}^{*\prime}(\mathcal{J}_5) - \frac{1}{2\xi} = 0$$

The expressions for the first Piola–Kirchhoff stress $\mathbf{S}$ and Lagrangian electric field $\mathbf{E}$ that the above relations entail with Eq. (6) read as

$$\mathbf{S} = \nu(z)\mathbf{F} - q\mathbf{F}^{-T} + \frac{1}{\omega(z,\xi)(1+\rho^3+\rho^2 I_2+\rho I_1)} \times \left[\rho(I_5^D\mathbf{F} - \mathbf{FD}\otimes\mathbf{F}^T\mathbf{FD} - \mathbf{FF}^T\mathbf{FD}\otimes\mathbf{D}) + (1+\rho I_1)\mathbf{FD}\otimes\mathbf{D}\right] - \frac{\rho I_5^D + \rho^3 I_4^D + \rho^2(I_1 I_5^D - I_6^D)}{\omega(z,\xi)(1+\rho^3+\rho^2 I_2+\rho I_1)^2}\left[\mathbf{F} - \rho\mathbf{F}^{-T}\mathbf{F}^{-1}\mathbf{F}^{-T}\right]$$

and

$$\mathbf{E} = \frac{1}{\omega(z,\xi)(1+\rho^3+\rho^2 I_2+\rho I_1)} \times \left[(1+\rho I_1)\mathbf{F}^T\mathbf{FD} + \rho^2\mathbf{D} - \rho\mathbf{F}^T\mathbf{FF}^T\mathbf{FD}\right]$$

in terms of the deformation gradient $\mathbf{F}$ and the Lagrangian electric displacement $\mathbf{D}$.

Remark 15 (Special cases of interest). A number of special cases of Eq. (30) are worth detailing explicitly.

As already mentioned in Sec. 1, expression (30) reduces to the result by Lefèvre and Lopez-Pamies [27] when the matrix is an ideal dielectric ($m_{\rm m} = \varepsilon_{\rm m}$). The free energy (30) shares its functional form with this earlier result—Eq. (56) in Ref. [27]—but thetwo results differ by the value taken by the electrostrictive coefficient m that depends explicitly on whether the apparent permittivity of the matrix is deformation-dependent, $m_{\rm m} \neq \varepsilon_{\rm m}$, or not $m_{\rm m} = \varepsilon_{\rm m}$.

In the case of a neo-Hookean matrix filled with ideal dielectric particles studied in Sec. 3, that is, for $\psi_{\rm m}(I_1) = \mu_{\rm m}/2$ in Eq. (28) and $\mathcal{S}_{\rm p}(I_5^E) = \varepsilon_{\rm p}/2$ in Eq. (29), the nonlinear algebraic equations (32) admit as exact solutions $z = \mu_{\rm m}$ and $\xi = \varepsilon_{\rm p}$ for arbitrary deformations and arbitrary electric fields. It follows that the free energy (30) reduces to the free energy (16) of Sec. 3 as expected.

For an arbitrary non-Gaussian matrix filled with *rigid* particles, that is, when $\mu_{\rm p} = \infty$, the coefficient $n(z)$ is linear in z while $\omega(z,\xi)$ is independent of z:

$$n(z) = (1-c)r(c)z, \quad \text{and} \quad \frac{\partial\omega}{\partial z}(z,\xi) = 0$$

with

$$r(c) = \frac{1}{5(1-c)|\Omega_0|}\int_{\Omega_0}[1-\theta_{\rm p}(\mathbf{X})]\mathcal{K}_{klmn}\Gamma_{mkl,n}\,{\rm d}\mathbf{X} \tag{38}$$

where $\mathbf{\Gamma}$ solution of Eq. (34) when $\mu_{\rm p} = \infty$. More simply put, the physical meaning of $n(z)$ entails that

$$n(z) = \frac{\mu z}{\mu_{\rm m}} \quad \text{and} \quad r(c) = \frac{\mu}{(1-c)\mu_{\rm m}} \tag{39}$$

with μ the shear modulus of the composite given by Eq. $(17)_1$ and $\mu_{\rm m} = 2\psi_{\rm m}'(3)$ the shear modulus of the matrix. It follows that $\mathcal{I}_1 = r(c)[I_1-3]+3$ and that equation $(32)_1$ admits the closed-form solution $z = 2\psi_{\rm m}'(r(c)[I_1-3]+3)$ which leads in turn to the incompressible free energy

$$W^r = (1-c)\psi_{\rm m}(r(c)[I_1-3]+3) - c\mathcal{S}_{\rm p}(\mathcal{I}_5) + \frac{c\xi}{2}\mathcal{I}_5 + \frac{\omega(\xi)-\nu(\xi)}{2}I_4^E - \frac{\omega(\xi)}{2}I_5^E \tag{40}$$

where, again, $\nu(\xi)$ and $\omega(\xi)$ are defined by Eq. $(33)_{2,3}$, $z = 2\psi_{\rm m}'(r(c)[I_1-3]+3)$, and ξ is solution of Eq. $(32)_2$. If in addition the particles are conductors, $\varepsilon_{\rm p} = \infty$, Eq. $(32)_2$ admits the closed-form solution $\xi = +\infty$ and the physical meaning of $\nu(\xi)$ and $\omega(\xi)$ leads to

$$\nu(\xi) = \varepsilon \quad \text{and} \quad \omega(\xi) = m \tag{41}$$

with ε and m the permittivity and dielectric coefficient of the composite at hand defined by $(17)_{2,3}$. It follows that the finite branch of Eq. (30) reduces to the *explicit* expression

$$W^{rc} = (1-c)\psi_{\rm m}\left(\frac{\mu}{(1-c)\mu_m}[I_1-3]+3\right) + \frac{m-\varepsilon}{2}I_4^E - \frac{m}{2}I_5^E \tag{42}$$

For an arbitrary non-Gaussian matrix filled with *liquid-like* particles, that is, when $\mu_{\rm p} = 0$, the coefficient $n(z)$ is linear in z while $\omega(z,\xi)$ is independent of z:

$$n(z) = (1-c)l(c)z \quad \text{and} \quad \frac{\partial\omega}{\partial z}(z,\xi) = 0$$

with

$$l(c) = \frac{1}{5(1-c)|\Omega_0|}\int_{\Omega_0}[1-\theta_{\rm p}(\mathbf{X})]\mathcal{K}_{klmn}\Gamma_{mkl,n}\,{\rm d}\mathbf{X} \tag{43}$$

where $\mathbf{\Gamma}$ solution of Eq. (34) when $\mu_{\rm p} = 0$. More simply put, the physical meaning of $n(z)$ entails as well that

$$n(z) = \frac{\mu z}{\mu_{\rm m}} \quad \text{and} \quad l(c) = \frac{\mu}{(1-c)\mu_{\rm m}} \tag{44}$$

with μ the shear modulus of the composite given by Eq. $(17)_1$ and $\mu_{\rm m} = 2\psi_{\rm m}'(3)$ the shear modulus of the matrix. It follows that $\mathcal{I}_1 = l(c)[I_1-3]+3$ and that Eq. $(32)_1$ admits the closed-form solution $z = 2\psi_{\rm m}'(l(c)[I_1-3]+3)$ which leads in turn to the incompressible free energy

$$W^l = (1-c)\psi_{\rm m}(l(c)[I_1-3]+3) - c\mathcal{S}_{\rm p}(\mathcal{I}_5) + \frac{c\xi}{2}\mathcal{I}_5 + \frac{\omega(\xi)-\nu(\xi)}{2}I_4^E - \frac{\omega(\xi)}{2}I_5^E \tag{45}$$

where, again, $\nu(\xi)$ and $\omega(\xi)$ are defined by Eq. $(33)_{2,3}$, $z = 2\psi_{\rm m}'(l(c)[I_1-3]+3)$, and ξ is solution of Eq. $(32)_2$. If here as well the particles are conductors, $\varepsilon_{\rm p} = \infty$, Eq. $(32)_2$ admits the closed-form solution $\xi = +\infty$ and the physical meaning of $\nu(\xi)$ and $\omega(\xi)$ leads to

$$\nu(\xi) = \varepsilon \quad \text{and} \quad \omega(\xi) = m \tag{46}$$

with ε and m the permittivity and dielectric coefficient of the composite at hand defined by $(17)_{2,3}$. It follows that the finite branch of (30) reduces to the *explicit* expression

$$W^{lc} = (1-c)\psi_{\rm m}\left(\frac{\mu}{(1-c)\mu_m}[I_1-3]+3\right) + \frac{m-\varepsilon}{2}I_4^E - \frac{m}{2}I_5^E \tag{47}$$

4.2 Isotropic Distribution of Spherical Particles.

Similar to Sec. 3.2, we report below the specialization of the general free energy (30)—and free energies (40) and (45)—to the practically relevant cases of dielectric elastomer composites comprising isotropic distributions of rigid- or liquid-like spherical particles.

4.2.1 Rigid Spherical Particles. For the case of rigid particles ($\mu_{\rm p} = \infty$), it follows from Remark 10 and Eq. (24) that the

coefficients $n(z)$, $\nu(\xi)$, and $\omega(\xi)$ are well approximated by

$$n(z)=(1-c)^{-5/2}z,\quad \nu(\xi)=\varepsilon_{\rm m}+\frac{3c(\xi-\varepsilon_{\rm m})\varepsilon_{\rm m}}{(2+c)\varepsilon_{\rm m}+(1-c)\xi}$$
$$\omega(\xi)=m_{\rm m}+\frac{3c(10+2c+3c^2)(\xi-\varepsilon_{\rm m})\varepsilon_{\rm m}m_{\rm m}}{5[(2+c)\varepsilon_{\rm m}+(1-c)\xi]^2}+\frac{3c(1-c)(5+3c)(\xi-\varepsilon_{\rm m})\xi m_{\rm m}}{5[(2+c)\varepsilon_{\rm m}+(1-c)\xi]^2} \tag{48}$$

for volume fractions of particles within the range $c\in[0,\,0.25]$ and for all values of the material parameters $\mu_{\rm m}$, $\varepsilon_{\rm m}$, $m_{\rm m}$, and ξ. Note that, as expected, the above expressions reduce to expressions (24) when $z=\mu_{\rm m}$ and $\xi=\varepsilon_{\rm p}$. The function $r(c)$ defined by Eqs. (38) and $(39)_2$ is then given by $r(c)=(1-c)^{-7/2}$ and it follows from Eqs. (31) and (48) that the finite branch of the free energy (40) reduces to

$$W^{r,\rm sph}=(1-c)\psi_{\rm m}\left(\frac{I_1-3}{(1-c)^{7/2}}+3\right)-c\mathcal{S}_{\rm p}\left(\mathcal{I}_5^{r,\rm sph}\right)+\frac{c\xi}{2}\mathcal{I}_5^{r,\rm sph}+\frac{\omega(\xi)-\nu(\xi)}{2}I_4^E-\frac{\omega(\xi)}{2}I_5^E \tag{49}$$

where $\nu(\xi)$ and $\omega(\xi)$ are given by Eq. $(48)_{2,3}$,

$$\mathcal{I}_5^{r,\rm sph}=\frac{9\varepsilon_{\rm m}^2}{[(2+c)\varepsilon_{\rm m}+(1-c)\xi]^2}I_4^E-9\varepsilon_{\rm m}m_{\rm m}[I_4^E-I_5^E]\times\frac{(5+c-6c^2)\xi+(10-c+6c^2)\varepsilon_{\rm m}}{[(2+c)\varepsilon_{\rm m}+(1-c)\xi]^3} \tag{50}$$

and the variable ξ is defined implicitly as the solution of the nonlinear algebraic equation $2\mathcal{S}_{\rm p}'(\mathcal{I}_5^{r,\rm sph})-\xi=0$.

For the limiting case when the spherical particles are electric conductors, the variable ξ is given explicitly by $\xi=+\infty$ and Eq. (49) reduces to

$$W^{rc,\rm sph}=(1-c)\psi_{\rm m}\left(\frac{I_1-3}{(1-c)^{7/2}}+3\right)-\frac{(1+2c)\varepsilon_{\rm m}}{2(1-c)}I_4^E+\frac{(5+10c+9c^2)m_{\rm m}}{10(1-c)}[I_4^E-I_5^E]$$

4.2.2 Liquid-Like Spherical Particles. For the case when the particles are liquid-like ($\mu_{\rm p}=0$), Remark 10 with Eq. (26) entails that the coefficients $n(z)$, $\nu(\xi)$, and $\omega(\xi)$ defined by Eq. (33) are well approximated by

$$n(z)=(1-c)^{5/3}z,\quad \nu(\xi)=\varepsilon_{\rm m}+\frac{3c(\xi-\varepsilon_{\rm m})\varepsilon_{\rm m}}{(2+c)\varepsilon_{\rm m}+(1-c)\xi}$$
$$\omega(\xi)=m_{\rm m}+\frac{c^2\left(400-729c^{11/25}\right)(\xi-\varepsilon_{\rm m})^2\varepsilon_{\rm m}}{500[(2+c)\varepsilon_{\rm m}+(1-c)\xi]^2}+\frac{3c\varepsilon_{\rm m}(5\varepsilon_{\rm m}\xi-3\varepsilon_{\rm m}m_{\rm m}-2\xi m_{\rm m})}{[(2+c)\varepsilon_{\rm m}+(1-c)\xi]^2} \tag{51}$$

for volume fractions of particles within the range $c\in[0,\,0.25]$ and for all values of the material parameters $\mu_{\rm m}$, $\varepsilon_{\rm m}$, $m_{\rm m}$, and ξ. Note that, as expected, the above expressions reduce to expressions (26) when $z=\mu_{\rm m}$ and $\xi=\varepsilon_{\rm p}$. The function $l(c)$ defined by Eqs. (43) and $(44)_2$ is then given by $l(c)=(1-c)^{2/3}$, and it follows from Eqs. (31) and (51) that the finite branch of the free energy (45) reduces to

$$W^{l,\rm sph}=(1-c)\psi_{\rm m}\left((1-c)^{2/3}[I_1-3]+3\right)-c\mathcal{S}_{\rm p}\left(\mathcal{I}_5^{l,\rm sph}\right)+\frac{c\xi}{2}\mathcal{I}_5^{l,\rm sph}+\frac{\omega(\xi)-\nu(\xi)}{2}I_4^E-\frac{\omega(\xi)}{2}I_5^E \tag{52}$$

where $\nu(\xi)$ and $\omega(\xi)$ are given by Eq. $(51)_{2,3}$,

$$\mathcal{I}_5^{l,\rm sph}=\frac{9\varepsilon_{\rm m}^2}{[(2+c)\varepsilon_{\rm m}+(1-c)\xi]^2}I_4^E-3\varepsilon_{\rm m}[I_4^E-I_5^E]\times\left[\frac{2[(1-4c)\varepsilon_{\rm m}+(1-c)\xi]m_{\rm m}}{[(2+c)\varepsilon_{\rm m}+(1-c)\xi]^3}+\frac{(5000-3700c+2187c^{36/25}-2500c^2)\varepsilon_{\rm m}^2}{250(1-c)[(2+c)\varepsilon_{\rm m}+(1-c)\xi]^3}-\frac{(1250-1650c+729c^{36/25})\varepsilon_{\rm m}}{250(1-c)[(2+c)\varepsilon_{\rm m}+(1-c)\xi]^2}\right] \tag{53}$$

and the variable ξ is defined implicitly as the solution of the nonlinear algebraic equation

$$2\mathcal{S}_{\rm p}'(\mathcal{I}_5^{l,\rm sph})-\xi=0 \tag{54}$$

For the limiting case when the particles are electrically conducting, the variable ξ is given explicitly by $\xi=+\infty$ and Eq. (52) reduces to

$$W^{lc,\rm sph}=(1-c)\psi_{\rm m}\left((1-c)^{2/3}[I_1-3]+3\right)-\frac{5(1+2c)\varepsilon_{\rm m}}{10(1-c)}I_4^E+\left[m_{\rm m}+\frac{(400-729c^{11/25})c^2\varepsilon_{\rm m}}{500(1-c)^2}\right][I_4^E-I_5^E]$$

4.2.3 Accuracy Assessment. To assess the accuracy of the free energies (49) and (52) for arbitrary deformations and electric fields, we report comparisons with full-field FE simulations, see Refs. [26,27] for details about these simulations. These comparisons also probe the specific functional form of Eqs. (49) and (52), that is, their independence on the invariants I_2 and I_6^E. Similarly to Sec. 3.2, this is achieved by following electromechanical loading paths along which four of the five isotropic invariants I_1, I_2, I_4^E, I_5^E, I_6^E are held constant while either I_2 or I_6^E is varied.

These results are reported in Fig. 5 and correspond to a dielectric elastomer matrix with free energy (28) and elasticity characterized by the Lopez-Pamies model [34]

$$\psi_{\rm m}(I_1)=\frac{3^{1-\alpha_1}}{2\alpha_1}\mu_1\left[I_1^{\alpha_1}-3^{\alpha_1}\right]+\frac{3^{1-\alpha_2}}{2\alpha_2}\mu_2\left[I_1^{\alpha_2}-3^{\alpha_2}\right] \tag{55}$$

The material parameters μ_1, μ_2, α_1, α_2, $\varepsilon_{\rm m}$, $m_{\rm m}$ that enter in the resulting free energy are listed in Table 1 and have been calibrated to experimental data for both the mechanical response of VHB 4910 under uniaxial tension [43] and for its longitudinal apparent permittivity when subjected to a biaxial pre-stretch [13]. Note that under a uniaxial loading $\mathbf{F}=\mathrm{diag}(\lambda^{-1/2},\,\lambda^{-1/2},\,\lambda)$ and in the absence of an electric field $\mathbf{E}=\mathbf{0}$, the uniaxial stress S_{un} implied by Eq. $(5)_1$ with Eqs. (28) and (55) reads as

$$S_{un}=\frac{\lambda^3-1}{2\lambda+\lambda^4}\sum_{r=1}^{2}3^{1-\alpha_r}\mu_r(\lambda^2+2\lambda^{-1})^{\alpha_r} \tag{56}$$

while the through-thickness deformation-dependent apparent permittivity $\widehat{\varepsilon}_{\rm m}$ of a thin film of dielectric elastomer with free energy (28) subjected to a biaxial stretch λ_b is given by[2]

$$\widehat{\varepsilon}_{\rm m}=m_{\rm m}+(\varepsilon_{\rm m}-m_{\rm m})\lambda_b^{-4} \tag{57}$$

Comparisons between the model (28) and (55), that is, the uniaxial stress (56) and apparent permittivity (57) and the experimental data of Hossain et al. [43] and Qiang et al. [13] are shown in Fig. 4 for illustrative purposes. It is clear from Fig. 4 that the choice of free

[2]This scalar deformation-dependent apparent permittivity $\widehat{\varepsilon}_{\rm m}$ of interest corresponds to the projection $\widehat{\varepsilon}_{\rm m}=\mathbf{n}\cdot\widehat{\boldsymbol{\varepsilon}}_{\rm m}(\mathbf{F})\mathbf{n}$ of the tensorial apparent permittivity $\widehat{\boldsymbol{\varepsilon}}_{\rm m}$ given by Eq. (4) when undergoing the biaxial stretch $\mathbf{F}=\lambda_b[\mathbf{I}-\mathbf{n}\otimes\mathbf{n}]+\lambda_b^{-2}\,\mathbf{n}\otimes\mathbf{n}$. Here, $\mathbf{n}$ stands for the normal of the thin film.

Table 1 Material parameters μ_1, μ_2, α_1, α_2, ε_m, m_m in the free-energy function (28) with (55) fitted to the electromechanical response of model VHB 4910 [13,43,44]

VHB 4910	
$\mu_1 = 13.54\,\text{kPa}$	$\mu_2 = 1.08\,\text{kPa}$
$\alpha_1 = 1.00$	$\alpha_2 = -2.474$
$\varepsilon_m = 4.52\,\varepsilon_0$	$m_m = 2.80\,\varepsilon_0$

energy (28) with (55) and material parameters listed in Table 1 provides an accurate model for the standard dielectric elastomer VHB 4910 by 3M over a large range of deformations and electric fields.

Furthermore, for all the results shown in Fig. 5, the elastic dielectric behavior of the particles is characterized by the free energy(29) with

$$\mathcal{S}_p(I_5^E) = \frac{\varepsilon_0}{2} I_5^E - \frac{(p_p^s)^2}{3(\varepsilon_p - \varepsilon_0)} \left[\ln\left(\frac{3(\varepsilon_p - \varepsilon_0)\sqrt{I_5^E}}{p_p^s} \right) - \ln\left(\sinh\left(\frac{3(\varepsilon_p - \varepsilon_0)\sqrt{I_5^E}}{p_p^s} \right) \right) \right] \tag{58}$$

and material parameters μ_p, ε_p, and p_p^s listed in Table 2. These material parameters correspond to the cases of rigid conducting particles, rigid high-permittivity particles with polarization saturation, and liquid-like conducting particles, representative of filler particles that have been utilized in a number of experiments [14–18,20,21].

Now, within the class of dielectric elastomer composites of interest here, Figs. 5(*a*) and 5(*b*) correspond to the case of a volume fraction $c = 0.05$ of rigid conducting particles, Figs. 5(*c*) and 5(*d*) correspond to the case of a volume fraction $c = 0.05$ of rigid high-permittivity particles with polarization saturation, and Figs. 5(*e*) and 5(*f*) correspond to the case a volume fraction $c = 0.15$ of liquid-like conducting particles. It is plain from Fig. 5 that the free energies (49) and (52) are in good quantitative agreement with the corresponding FE simulations for all three types of particles. It is also clear that the FE simulations are by and large independent of I_2 or I_6^E, as are the free energies (49) and (52). Similar comparisons for a wide range of choices for $\psi_m(I_1)$, ε_m, m_m, $\mathcal{S}_p(I_5^E)$, and ε_p, not included here for conciseness, have shown that the free energies (49) and (52) are good quantitative approximations of the free energy of non-Gaussian elastomers with deformation-dependent apparent permittivity, characterized by Eq. (28), filled with isotropic distributions of rigid or liquid particles, characterized by Eq. (29) with either $\mu_p = \infty$ or $\mu_p = 0$.

5 Electrostrictive Response of Dielectric Elastomer Composites With Deformation-Dependent Apparent-Permittivity Matrix

In this final section, we deploy the proposed constitutive model to probe the electrostrictive response of dielectric elastomer composites comprising a matrix with deformation-dependent apparent permittivity. Results pertaining to arbitrary isotropic, two-phase, non-percolative particulate microstructures are reported in Sec. 5.1 while corresponding specializations to the practically relevant cases of rigid or liquid-like spherical particles are recorded in Sec. 5.2. This section also contains results for three different classes of dielectric elastomer composites, all made out of a VHB 4910 matrix filled either by rigid conducting particles, rigid high-permittivity particles with polarization saturation, or liquid-like conducting particles. Finally, in an effort to further highlight the generality of the proposed model and its usage for composites comprising particles that are not spherical in shape, results for an isotropic distribution of randomly oriented rigid conducting spheroidal particles are included in Sec. 5.3.

5.1 Arbitrary Isotropic, Two-Phase, Non-percolative Particulate Microstructure. The prototypical experimental setup utilized to probe the coupled electromechanical response of stretchable dielectrics consists in measuring the compressive deformation—or electrostriction—undergone when subjected to a uniform electric field in the absence of stresses. This is typically achieved by layering a thin and flat specimen of the active material between deformable electrodes connected to an external battery. Consider then the electromechanical states of a thin specimen subjected to prescribed first Piola–Kirchoff stress $\mathbf{S}$ and Lagrangian electric field $\mathbf{E}$ of the form[3]

$$\mathbf{S} = \mathbf{0} \quad \text{and} \quad \mathbf{E} = E\mathbf{n} \tag{59}$$

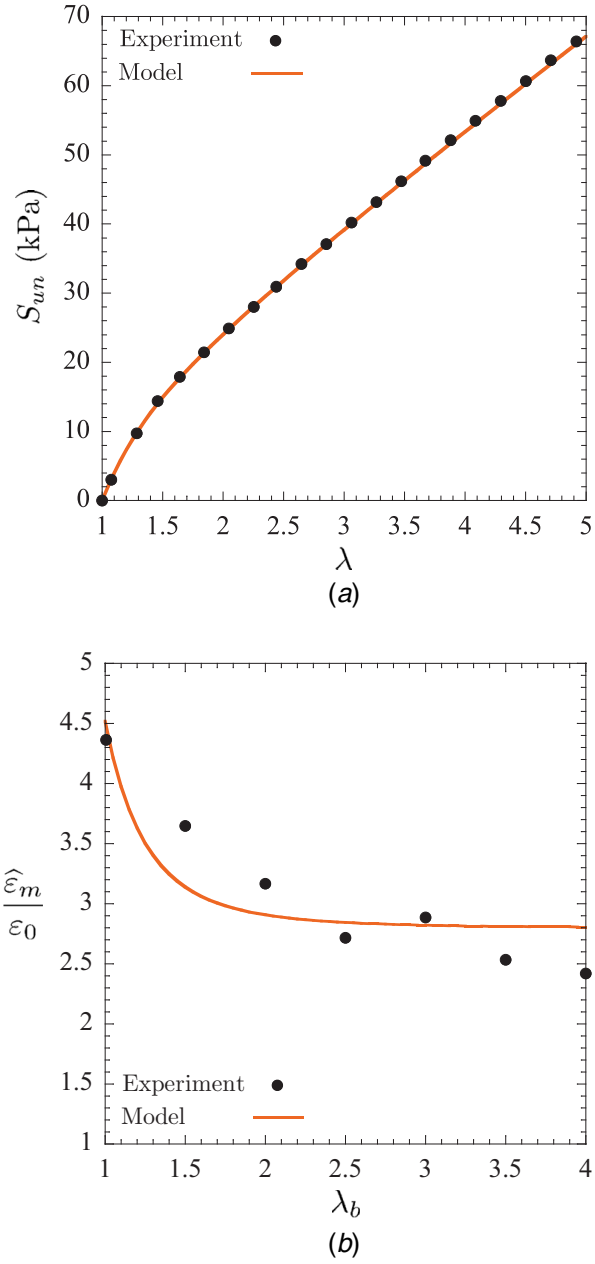

Fig. 4 The model (28) with (55) and the material parameters of Table 1 compared with experimental data for the standard dielectric elastomer VHB 4910: (*a*) uniaxial stress-stretch response in the absence of electric fields (56) compared with the experimental data of Hossain et al. [43], (*b*) through-thickness deformation-dependent apparent permittivity of a biaxially pre-stretched thin film (57) compared with the experimental data of Qiang et al. [13]

[3]Given the thinness of the specimen and fashion in which the external electric field is applied, it is reasonable to assume that there are no electric fields in the air surrounding the specimen.

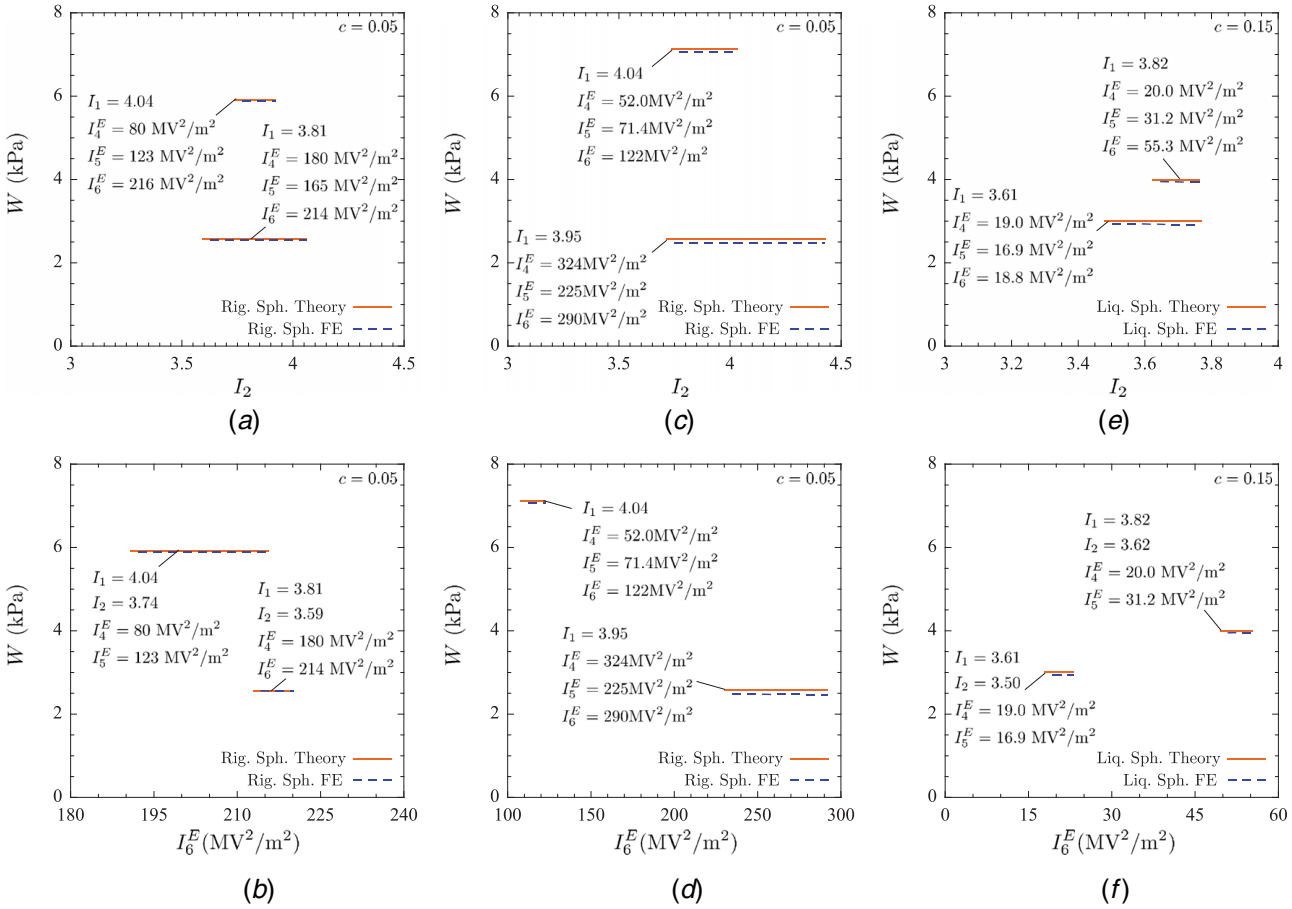

Fig. 5 Plots of the free energy W of a typical dielectric elastomer—described by the free energy (28) with (55) and material parameters listed in Table 1—filled with (*a*) and (*b*) a volume fraction $c = 0.05$ of rigid conducting particles, (c) and (*d*) a volume fraction $c = 0.05$ of rigid high-permittivity particles with polarization saturation, and (e) and (*f*) a volume fraction $c = 0.15$ of liquid-like conducting particles, described by the free energy (29) with (58) and material parameters listed in Table 2. The solid lines ("Rig. Sph. Theory" and "Liq. Sph. Theory") correspond to expressions (49) and (52) while the dashed lines ("Rig. Sph. FE" and "Liq. Sph. FE") correspond to full-field FE simulations.

Table 2 Material parameters μ_p, ε_p, and p_p^s in the free-energy function (29) with (58) chosen to represent rigid conducting particles, rigid high-permittivity particles with polarization saturation, and liquid-like conducting particles

Rigid conducting particles	Rigid high-permittivity particles with polarization saturation	Liquid-like conducting particles
$\mu_p = \infty$	$\mu_p = \infty$	$\mu_p = \infty$
$\varepsilon_p = \infty$	$\varepsilon_p = 100\,\varepsilon_0$	$\varepsilon_p = \infty$
$p_p^s = \infty$	$p_p^s = 10^{-4}\ \mathrm{C/m^2}$	$p_p^s = \infty$

with $\mathbf{n}$ the normal of the thin specimen. The constitutive relations (36) entail that the deformation gradient $\mathbf{F}$ and Lagrangian electric displacement $\mathbf{D}$ are of the form

$$\mathbf{F} = \lambda^{-1/2}[\mathbf{I} - \mathbf{n}\otimes\mathbf{n}] + \lambda\mathbf{n}\otimes\mathbf{n} \quad \text{and} \quad \mathbf{D} = D\mathbf{n} \tag{60}$$

with their non-trivial components defined by

$$\lambda^4 - \lambda + \frac{\omega(z,\,\xi)}{n(z)}E^2 = 0 \quad \text{and}$$
$$D = \left[\nu(\xi) - \omega(z,\,\xi)\left(1 - \frac{1}{\lambda^2}\right)\right]E \tag{61}$$

The above expressions fully characterize the electrostrictive response under conditions (59) of a non-Gaussian dielectric elastomer with deformation-dependent apparent permittivity with free energy (28) filled with any isotropic non-percolative distribution of particles characterized by the free energy (29). We recall here that $n(z)$, $\nu(\xi)$, and $\omega(z,\,\xi)$ are defined by Eq. (33) with the variables z and ξ solutions of the nonlinear algebraic equations (32) with (31) where here, $I_1 = \lambda^2 + 2\lambda^{-1}$, $I_4 = E^2$, and $I_5 = \lambda^{-2}E^2$. It follows from Eq. $(8)_{2,3}$ that Eq. $(61)_2$ can be rewritten as

$$d = \left[\lambda^2\nu(\xi) + \left(1 - \lambda^2\right)\omega(z,\,\xi)\right]e \tag{62}$$

in terms of the non-trivial components of the Eulerian electric field $\mathbf{e} = e\mathbf{n} = \lambda^{-1}E\mathbf{n}$ and Eulerian electric displacement $\mathbf{d} = d\mathbf{n} = \lambda D\mathbf{n}$. It is then apparent that $\widehat{\varepsilon}(\lambda,\,e) = \lambda^2\nu(\xi) + \left(1 - \lambda^2\right)\omega(z,\,\xi)$ corresponds to the apparent permittivity of the dielectric elastomer composite under electrostriction loading (59).

5.2 Isotropic Distribution of Spherical Particles. While the above expressions are quite general, we spell below out their specializations to the cases of dielectric elastomer composites comprising isotropic distributions of rigid- or liquid-like spherical particles.

5.2.1 Rigid Particles. For the case of rigid particles ($\mu_p = \infty$), making use of Eq. (48) for $n(z)$, $\nu(\xi)$, and $\omega(\xi)$ and of $z =$

$2\psi'_{\rm m}((1-c)^{-7/2}[I_1-3]+3)$ in Eqs. $(61)_1$ and (62) leads to

$$\lambda^4-\lambda+\frac{(1-c)^{5/2}\omega(\xi)}{2\psi'_{\rm m}\left(\dfrac{\lambda^2+2\lambda^{-1}-3}{(1-c)^{7/2}}+3\right)}E^2=0$$
$$\text{and}\quad d=\left[\lambda^2\nu(\xi)+\left(1-\lambda^2\right)\omega(\xi)\right]e \tag{63}$$

where it is recalled for completeness that $\nu(\xi)$ and $\omega(\xi)$ are given by

$$\nu(\xi)=\varepsilon_{\rm m}+\frac{3c(\xi-\varepsilon_{\rm m})\varepsilon_{\rm m}}{(2+c)\varepsilon_{\rm m}+(1-c)\xi}$$
$$\omega(\xi)=m_{\rm m}+\frac{3c(10+2c+3c^2)(\xi-\varepsilon_{\rm m})\varepsilon_{\rm m}m_{\rm m}}{5[(2+c)\varepsilon_{\rm m}+(1-c)\xi]^2}+\frac{3c(1-c)(5+3c)(\xi-\varepsilon_{\rm m})\xi m_{\rm m}}{5[(2+c)\varepsilon_{\rm m}+(1-c)\xi]^2}$$

the variable ξ is defined implicitly as the solution of the nonlinear algebraic equation $2\mathcal{S}'_{\rm p}(\mathcal{I}_5^{r,\rm sph})-\xi=0$ with Eq. (50) reading here as

$$\mathcal{I}_5^{r,\rm sph}=\frac{9\varepsilon_{\rm m}^2}{[(2+c)\varepsilon_{\rm m}+(1-c)\xi]^2}E^2-9\varepsilon_{\rm m}m_{\rm m}[1-\lambda^{-2}]E^2\times\frac{(5+c-6c^2)\xi+(10-c+6c^2)\varepsilon_{\rm m}}{[(2+c)\varepsilon_{\rm m}+(1-c)\xi]^3}$$

and $e=\lambda^{-1}E$. We emphasize here that the above expressions are valid for arbitrary choices of functions $\psi_{\rm m}(I_1)$ and $\mathcal{S}_{\rm p}(I_5^E)$ in Eqs. (28) and (29) to describe the non-Gaussian elasticity of the dielectric elastomer matrix and the dielectric response of the rigid particles.

In the limiting case when the particles are electrically conducting, the variable ξ is given explicitly by $\xi=+\infty$ and the electrostriction response (63) reduces to

$$\lambda^4-\lambda+\frac{(1-c)^{3/2}(5+10c+9c^2)m_{\rm m}}{10\psi'_{\rm m}\left(\dfrac{\lambda^2+2\lambda^{-1}-3}{(1-c)^{7/2}}+3\right)}E^2=0$$
$$\text{and}\quad d=\left[\lambda^2\frac{(1+2c)\varepsilon_{\rm m}}{(1-c)}+\left(1-\lambda^2\right)\frac{(5+10c+9c^2)m_{\rm m}}{5(1-c)}\right]e \tag{64}$$

5.2.2 Liquid-Like Particles. For the case of liquid-like particles ($\mu_{\rm p}=0$), making use of Eq. (51) for $n(z)$, $\nu(\xi)$, and $\omega(\xi)$ and of $z=2\psi'_{\rm m}((1-c)^{2/3}[I_1-3]+3)$ in Eqs. $(61)_1$ and (62) leads to

$$\lambda^4-\lambda+\frac{(1-c)^{-5/3}\omega(\xi)}{2\psi'_{\rm m}((1-c)^{2/3}[\lambda^2+2\lambda^{-1}-3]+3)}E^2=0$$
$$\text{and}\quad d=\left[\lambda^2\nu(\xi)+\left(1-\lambda^2\right)\omega(\xi)\right]e \tag{65}$$

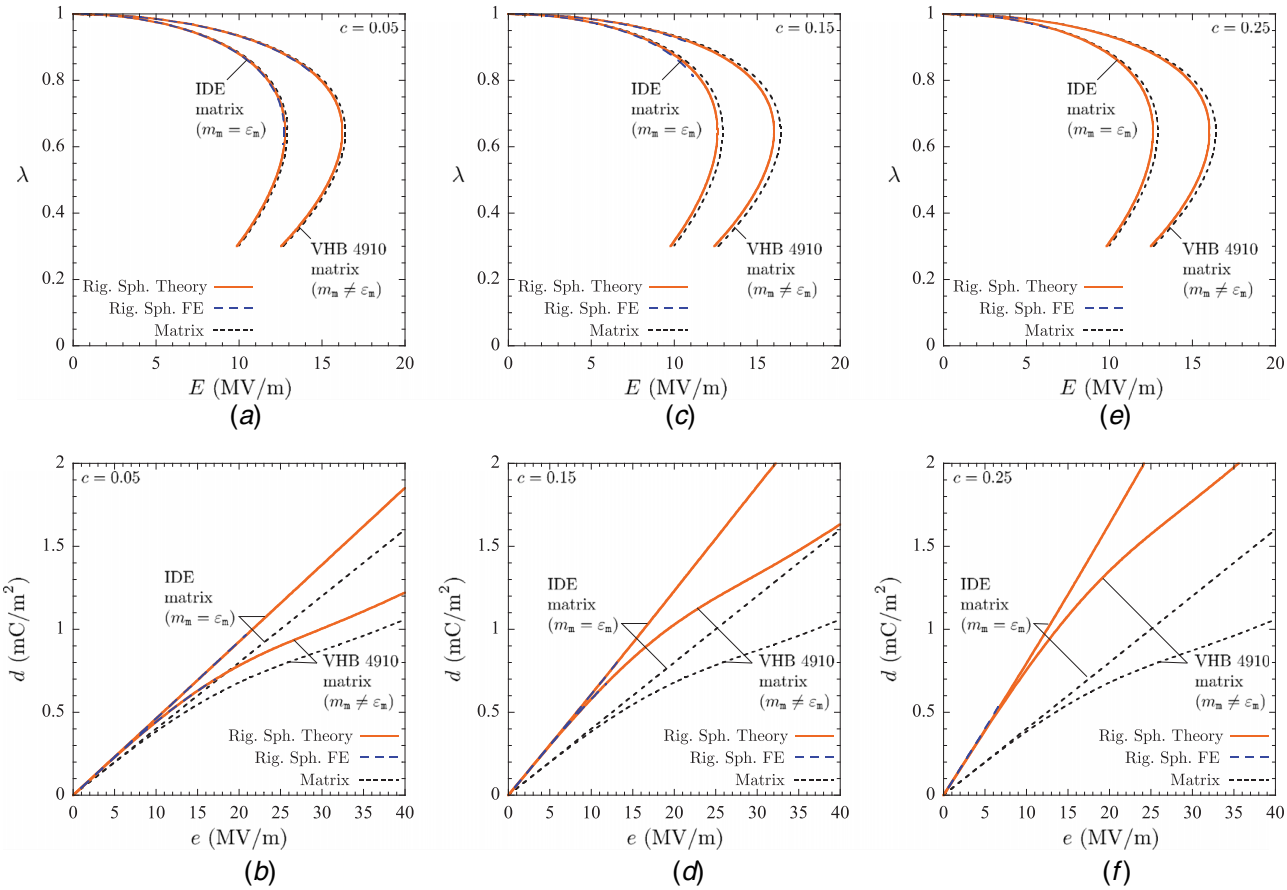

Fig. 6 Electrostriction and dielectric response—defined by (59)—of dielectric elastomer composites with volume fractions c = 0.05, 0.15, 0.25 of rigid conducting spherical particles described by the free energy (29) with (58) and material parameters listed in Table 2. Particles are isotropically dispersed in a dielectric elastomer, either VHB 4910, characterized by the free energy (28) with (55) and material parameters listed in Table 1 where $m_{\rm m}\neq\varepsilon_{\rm m}$, or the fictional ideal elastic dielectric elastomer IDE characterized by the free energy (28) with (55) and material parameters listed in Table 3 where $m_{\rm m}=\varepsilon_{\rm m}$. Solid lines ("Rig. Sph. Theory") correspond to the proposed model (64), dashed lines ("Rig. Sph. FE") correspond to full-field FE simulations, and dotted lines corresponds to the unfilled VHB 4910 and IDE matrix (c = 0).

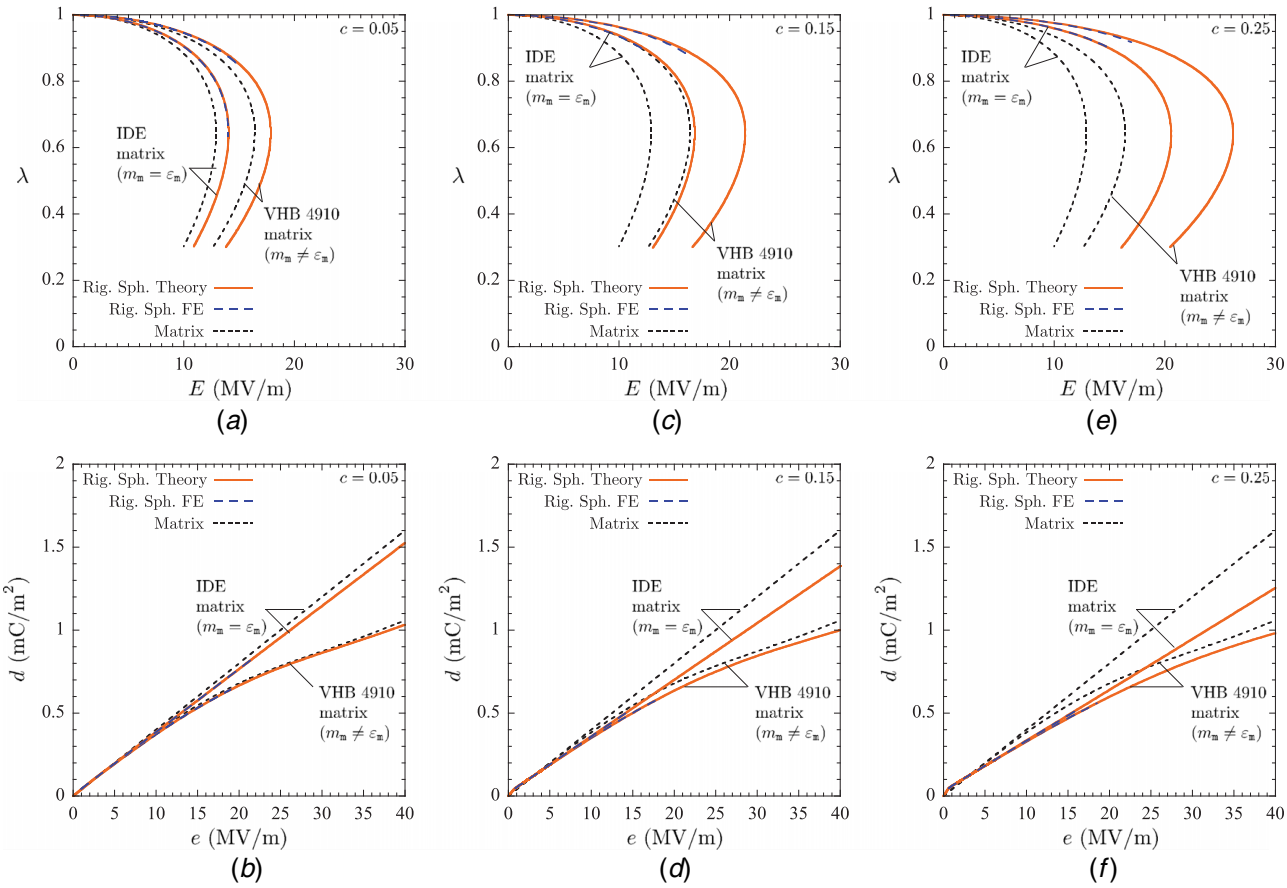

Fig. 7 Electrostriction and dielectric response—defined by (59)—of dielectric elastomer composites with volume fractions $c = 0.05, 0.15, 0.25$ of rigid high-permittivity spherical particles with polarization saturation described by the free energy (29) with (58) and material parameters listed in Table 2. Particles are isotropically dispersed in a dielectric elastomer, either VHB 4910, characterized by the free energy (28) with (55) and material parameters listed in Table 1 where $m_m \neq \varepsilon_m$, or the fictional ideal elastic dielectric elastomer IDE characterized by the free energy (28) with (55) and material parameters listed in Table 3 where $m_m = \varepsilon_m$. Solid lines ("Rig. Sph. Theory") correspond to the proposed model (63), dashed lines ("Rig. Sph. FE") correspond to full-field FE simulations, and dotted lines corresponds to the unfilled VHB 4910 and IDE matrix ($c = 0$).

where it is recalled for completeness that $\nu(\xi)$ and $\omega(\xi)$ are in this case given by

$$\nu(\xi) = \varepsilon_m + \frac{3c(\xi - \varepsilon_m)\varepsilon_m}{(2+c)\varepsilon_m + (1-c)\xi}$$

$$\omega(\xi) = m_m + \frac{c^2\left(400 - 729c^{11/25}\right)(\xi - \varepsilon_m)^2\varepsilon_m}{500[(2+c)\varepsilon_m + (1-c)\xi]^2} + \frac{3c\varepsilon_m(5\varepsilon_m\xi - 3\varepsilon_m m_m - 2\xi m_m)}{[(2+c)\varepsilon_m + (1-c)\xi]^2}$$

the variable ξ is defined implicitly as the solution of the nonlinear algebraic equation $2\mathcal{S}_p'(\mathcal{I}_5^{l,\mathrm{sph}}) - \xi = 0$ with Eq. (53) reading here as

$$\mathcal{I}_5^{l,\mathrm{sph}} = \frac{9\varepsilon_m^2}{[(2+c)\varepsilon_m + (1-c)\xi]^2}E^2 - 3\varepsilon_m[1-\lambda^{-2}]E^2 \times \left[\frac{2[(1-4c)\varepsilon_m + (1-c)\xi]m_m}{[(2+c)\varepsilon_m + (1-c)\xi]^3} + \frac{(5000 - 3700c + 2187c^{36/25} - 2500c^2)\varepsilon_m^2}{250(1-c)[(2+c)\varepsilon_m + (1-c)\xi]^3} - \frac{(1250 - 1650c + 729c^{36/25})\varepsilon_m}{250(1-c)[(2+c)\varepsilon_m + (1-c)\xi]^2}\right]$$

and $e = \lambda^{-1}E$. We emphasize here that the above expressions are valid for arbitrary choices of functions $\psi_m(I_1)$ and $\mathcal{S}_p(I_5^E)$ in Eqs. (28) and (29) to describe the non-Gaussian elasticity of the dielectric elastomer matrix and the dielectric response of the liquid-like particles.

In the limiting case when the particles are electrically conducting, the variable ξ is given explicitly by $\xi = +\infty$ and the electrostriction response (65) reduces to

$$\lambda^4 - \lambda + \frac{(1-c)^{-5/3}\left[m_m + \frac{(400 - 729c^{11/25})c^2\varepsilon_m}{500(1-c)^2}\right]}{2\psi_m'\left((1-c)^{2/3}[\lambda^2 + 2\lambda^{-1} - 3] + 3\right)}E^2 = 0 \quad \text{and}$$

$$d = \left[\lambda^2\frac{(1+2c)\varepsilon_m}{(1-c)} + (1-\lambda^2) \times \left(m_m + \frac{(400 - 729c^{11/25})c^2\varepsilon_m}{500(1-c)^2}\right)\right]e \qquad (66)$$

5.2.3 Electrostriction Response. Sample results for the electrostrictive response—defined by Eq. (59)—of three different classes of dielectric elastomer composites composed of a VHB 4910 matrix filled by either rigid conducting spherical particles, rigid high-permittivity spherical particles with polarization saturation, or liquid-like conducting spherical particles, are presented, labeled as "VHB 4910 matrix ($m_m \neq \varepsilon_m$)," in Figs. 6–8, respectively. A second set of results, identified as "IDE matrix($m_m = \varepsilon_m$)," is included in Figs. 6–8 to illustrate the influence of the deformation-dependent apparent permittivity of the matrix on the response of the composite. These results pertain to the same classes of dielectric elastomer composites that now comprise as matrix phase an ideal dielectric elastomer that exhibits the same elastic response as VHB 4910 but with a deformation-*independent* apparent permittivity equal in value to the

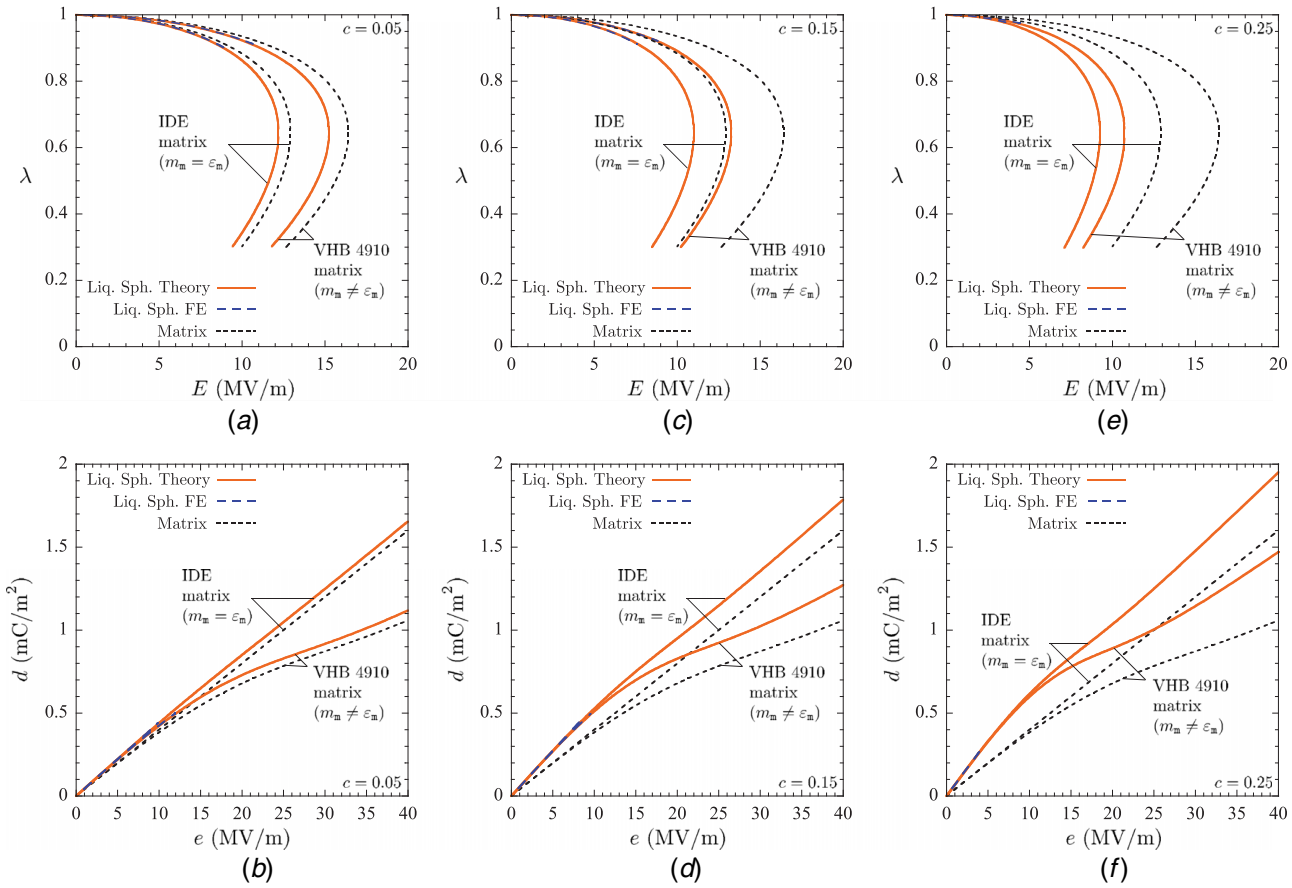

Fig. 8 Electrostriction and dielectric response—defined by (59)—of dielectric elastomer composites with volume fractions $c = 0.05, 0.15, 0.25$ of liquid-like conducting spherical particles described by the free energy (29) with (58) and material parameters listed in Table 2. Particles are isotropically dispersed in a dielectric elastomer, either VHB 4910, characterized by the free energy (28) with (55) and material parameters listed in Table 1 where $m_m \neq \varepsilon_m$, or the fictional ideal elastic dielectric elastomer IDE characterized by the free energy (28) with (55) and material parameters listed in Table 3 where $m_m = \varepsilon_m$. Solid lines ("Liq. Sph. Theory") correspond to the proposed model (66), dashed lines ("Liq. Sph. FE") correspond to full-field FE simulations, and dotted lines corresponds to the unfilled VHB 4910 and IDE matrix ($c = 0$).

permittivity of VHB 4910, $\varepsilon_m = m_m = 4.48\,\varepsilon_0$. This fictional ideal dielectric elastomer is referred to as "IDE" and the material parameters that describe its electromechanical response (28) with (55) are listed in Table 3 for completeness.

More specifically, for all results shown in Figs. 6–8, the elastic dielectric response of the VHB 4910 (IDE) matrix is described by the free energy (28) with (55) and the choice of material properties listed in Table 1 (Table 3), while the dielectric elastic response of the three types of particles is described by the free energy (29) with (58) and the corresponding choices of material properties listed in Table 2. Parts (*a*), (*c*), and (*e*) of Figs. 6–8 show the compressive electrostriction deformation λ of these dielectric elastomer composites as a function of the applied Lagrangian electric field E, while parts (*b*), (*d*), and (*f*) show their dielectric response in its Eulerian form. Results presented with a solid line in Figs. 6–8 correspond to the proposed model given by Eqs. (64),(63), and (66) for three volume fractions $c = 0.05$, $c = 0.15$, $c = 0.25$ of particles. Corresponding FE results for isotropic distributions of monodisperse spherical inclusions are also included with a dashed line to further illustrate the accuracy of the proposed model, see Ref. [27] for details. Results pertaining to the unfilled VHB 4910 or IDE matrix ($c = 0$) are reported with a dotted line for comparison purposes.

A quick glance at Figs. 6–8 suffices to realize that whether the matrix is an ideal dielectric (IDE with $m_m = \varepsilon_m$) or not (VHB 4910 with $m_m \neq \varepsilon_m$) significantly impacts the electromechanical response of the three classes dielectric elastomer composites under scrutiny here. In particular, it is clear from parts (*a*), (*c*), and (*e*) of these figures that the deformation-dependent apparent permittivity of VHB 4910 significantly reduces its electrostriction and that of the corresponding composites when compared with the electrostriction of the IDE matrix and of its composites. It is also apparent from parts (*b*), (*d*), and (*f*) of these figures that the nature of the dielectric response of the VHB 4910 ($m_m \neq \varepsilon_m$) and IDE ($m_m = \varepsilon_m$) matrix materials significantly impacts the dielectric response of dielectric elastomer composites. Note that granted $(62)_2$, the slope of the curves in parts (*b*), (*d*), and (*f*) of Figs. 6–8 corresponds to the apparent permittivity of the material when undergoing electrostrictive deformations. It is then clear that the sensitivity of the apparent permittivity on the deformations of such composite undergoes strongly depends on whether the matrix is an ideal

Table 3 Material parameters μ_1, μ_2, α_1, α_2, ε_m, m_m in the free-energy function (28) with (55) of a fictional ideal dielectric elastomer IDE that exhibits the same elastic response as VHB 4910 and has a deformation-independent apparent permittivity equal in value to the permittivity of VHB 4910

IDE	
$\mu_1 = 13.54$ kPa	$\mu_2 = 1.08$ kPa
$\alpha_1 = 1.00$	$\alpha_2 = -2.474$
$\varepsilon_m = 4.52\,\varepsilon_0$	$m_m = 4.52\,\varepsilon_0$

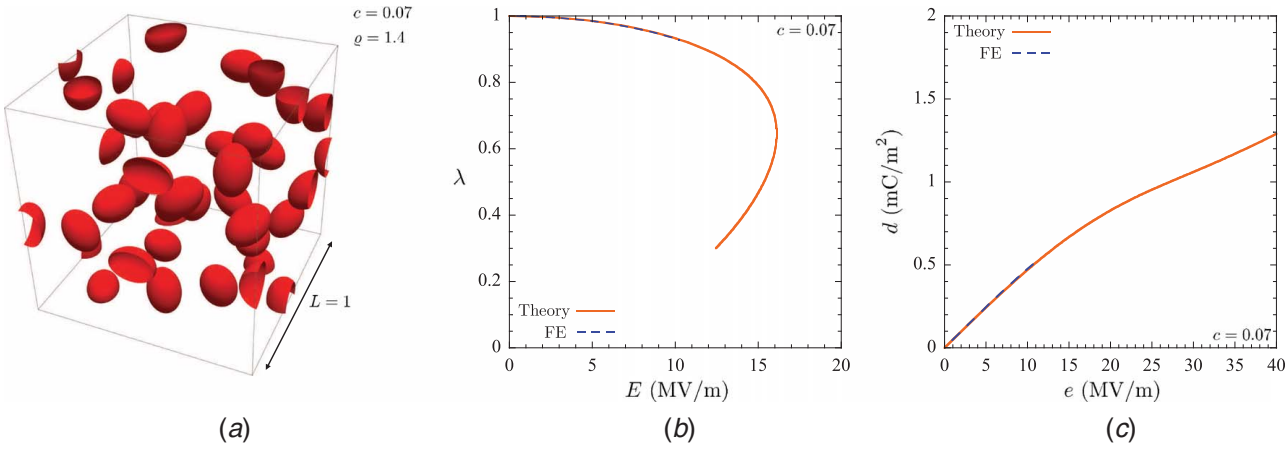

Fig. 9 Electrostriction and dielectric response—defined by (59)—of VHB 4910 isotropically filled with a volume fraction c = 0.07 of randomly oriented rigid conducting prolate spheroids with aspect ratio ϱ = 1.4. VHB 4910 is characterized by the free energy (28) with (55) and material parameters listed in Table 1 and the particles are described by the free energy (29) with (58) and material parameters listed in Table 2. Solid lines ("Theory") correspond to the proposed model (67) with (55) and the parameters in Table 4 while dashed lines ("FE") correspond to full-field FE simulations.

dielectric[4] ($m_m = \varepsilon_m$) or not ($m_m \neq \varepsilon_m$). This strong effect prompts appropriately accounting the deformation-dependent apparent-permittivity of dielectric elastomers in constitutive models describing dielectric elastomer composites they can be part of.

The results shown in Figs. 6–8 also provide direct insight into the effects of the addition of different types of particles to a dielectric elastomer with deformation-dependent apparent permittivity such as VHB 4910. It is plain for instance from the results of Fig. 6 that the isotropic addition of rigid conducting spherical particles to dielectric elastomers does not significantly changes their electrostriction but does increase their dielectric response. These results reveal the balance between the competing effects of increased stiffness ($n(z) > \mu_m$) and of increased dielectric ($\nu(\xi) > \varepsilon_m$) and electrostrictive ($\omega(\xi) > m_m$) properties. This is in contrast with available experimental results [16,20] which have been conjectured [27,45] to result from the presence of space charges at the lengthscale of the composites' microstructures.

On the contrary, results presented in Fig. 7 show that the isotropic addition of rigid high-permittivity spherical particles with polarization saturation significantly reduces the electrostriction and dielectric response of the material. In addition to the increased stiffness ($n(z) > \mu_m$), this stems from the fact that the magnitude of the applied electric field increases, the solution to the nonlinear algebraic equation $2\mathcal{S}_p'(\mathcal{I}_5) - \xi = 0$ decreases from $\xi = \varepsilon_p$ when $|\mathbf{E}| = 0$ to $\xi = \varepsilon_0$ in the limit of infinitely large electric fields, $|\mathbf{E}| \to \infty$. This leads via $\nu(\xi) < \varepsilon_m$ and $\omega(\xi) < m_m$ to the reduced electrostriction and dielectric response observed in Fig. 7.

Finally, results presented in Fig. 8 indicate that both the electrostriction and dielectric response of the matrix are enhanced by the addition of liquid-like conducting spherical particles. This is a result of the reduction in the stiffness of the material ($n(z) < \mu_m$) combined with its increased dielectric ($\nu(\xi) > \varepsilon_m$) and electrostrictive ($\omega(\xi) > m_m$) properties from the addition of soft conducting particles.

5.3 Isotropic Distribution of Randomly Oriented Rigid Conducting Spheroidal Particles. With the aim of further highlighting the use of the proposed framework for arbitrary isotropic, two-phase, non-percolative particulate microstructures, we report below sample results for the electrostrictive response of VHB 4910 filled with a volume fraction $c = 0.07$ of randomly oriented rigid conducting prolate spheroidal particles with aspect ratio $\varrho = 1.4$, see Fig. 9(*a*) for the realization at hand. As above, VHB 4910 is taken to be characterized by the free energy(28) with (55) and material parameters listed in Table 1 while the particles are characterized by the free energy (29) with (58) and material parameters listed in Table 2.

Given that the particles are rigid and conductors, the macroscopic elastic dielectric response of the composite at hand is given by Eq. (42) and its electrostrictive response (61) and (62) reduces to

$$\lambda^4 - \lambda + \frac{\mu_m m}{2\mu\psi_m'\left(\dfrac{\mu}{(1-c)\mu_m}[\lambda^2 + 2\lambda^{-1} - 3] + 3\right)} E^2 = 0$$
$$\text{and} \quad d = \left[\lambda^2\varepsilon + \left(1-\lambda^2\right)m\right]e \tag{67}$$

The above expressions depend on the elastic response of the VHB 4910 matrix $\psi_m(I_1)$ given by (55) and its shear modulus $\mu_m = 2\psi_m'(3) = \mu_1 + \mu_2$, and on of the shear modulus μ, permittivity ε, and electrostrictive coefficient m of the composite at hand. The shear modulus μ, permittivity ε, and electrostrictive coefficient m of the present realization have been computed numerically according to their definitions (17)—see Remark 5 for details—and their values are reported in Table 4 with that of the shear modulus of the matrix μ_m. Figures 9(*b*) and 9(*c*) illustrate the good agreement between the electrostrictive response (67) with (55) and the parameters in Table 4, shown with a solid line, and that obtained from FE simulations plotted with a dashed line.

Table 4 Shear modulus μ, permittivity ε, and electrostrictive coefficient m of an isotropic distribution of a volume fraction c = 0.07 of randomly oriented rigid conducting prolate spheroids with aspect ratio ϱ = 1.4 in VHB 4910

Randomly oriented rigid conducting prolate spheroids in VHB 4910		
$\mu_m = 14.62$ kPa	$c = 0.07$	
$\mu = 17.31$ kPa	$\varepsilon = 5.55\ \varepsilon_0$	$m = 3.42\ \varepsilon_0$

[4]Recall that a dielectric elastomer composite made out of an ideal dielectric matrix ($m_m = \varepsilon_m$) is not itself in general an ideal dielectric—see Remark 6—but note that this trait is very mild for the case of rigid particles but is much more apparent for the case of liquid-like particles, see, e.g., Figs. 6–8(*f*).

Acknowledgment

The support from the computational resources and staff contributions provided for the Quest high performance computing facility at Northwestern University, which is jointly supported by the Office of the Provost, the Office for Research, and Northwestern University Information Technology, is gratefully acknowledged. Access to the Quest high performance computing facility was made possible in part thanks to a Haythornthwaite Foundation Research Initiation Grant from the Applied Mechanics Division of the American Society of Mechanical Engineers.

Conflict of Interest

There are no conflicts of interest.

Data Availability Statement

The datasets generated and supporting the findings of this article are obtainable from the corresponding author upon reasonable request.

References

[1] Bar-Cohen, Y., 2001, *Electroactive Polymer (EAP) Actuators as Artificial Muscles*, SPIE Press, Bellingham, Washington.
[2] Carpi, F., and Smela, E., 2009, *Biomedical Applications of Electroactive Polymer Actuators*, John Wiley & Sons, Chichester, West Sussex.
[3] Kornbluh, R. D., Pelrine, R., Prahlad, H., Wong-Foy, A., McCoy, B., Kim, S., Eckerle, J., and Low, T., 2011, "From Boots to Buoys: Promises and Challenges of Dielectric Elastomer Energy Harvesting," Proc. SPIE 7976, Electroactive Polymer Actuators and Devices (EAPAD) 2011, **7976**.
[4] Liu, L., Liu, Y., and Leng, J., 2013, "Theory Progress and Applications of Dielectric Elastomers," Int. J. Smart Nano Mater., **4**(3), pp. 199–209.
[5] Bar-Cohen, Y., and Anderson, I. A., 2019, "Electroactive Polymer (EAP) Actuators—Background Review," Mech. Soft Mater., **1**(1), p. 5.
[6] Kofod, G., Sommer-Larsen, P., Kornbluh, R., and Pelrine, R., 2003, "Actuation Response of Polyacrylate Dielectric Elastomers," J. Intell. Mater. Syst. Struct., **14**(12), pp. 787–793.
[7] McKay, T. G., Calius, E., and Anderson, I. A., 2009, "The dielectric constant of 3M VHB: a parameter in dispute," Proc. SPIE 7287, Electroactive Polymer Actuators and Devices (EAPAD) 2009, **7287**.
[8] Di Lillo, L., Schmidt, A., Bergamini, A., Ermanni, P., and Mazza, E., 2011, "Dielectric and Insulating Properties of An Acrylic DEA Material At High Near-DC Electric Fields," Proc. SPIE 7976, Electroactive Polymer Actuators and Devices (EAPAD) 2011, **7976**.
[9] Cohen, N., Dayal, K., and DeBotton, G., 2016, "Electroelasticity of Polymer Networks," J. Mech. Phys. Solids, **92**, pp. 105–126.
[10] Choi, H. R., Jung, K., Chuc, N. H., Jung, M., Koo, I., Koo, J., Lee, J., Lee, J., Nam, J., Cho, M., and Lee, Y., 2005, "Effects of Prestrain on Behavior of Dielectric Elastomer Actuator," Proc. SPIE 5759, Smart Structures and Materials 2005: Electroactive Polymer Actuators and Devices (EAPAD), **5759**.
[11] Wissler, M., and Mazza, E., 2007, "Electromechanical Coupling in Dielectric Elastomer Actuators," Sens. Actuators., A, **138**(2), pp. 384–393.
[12] Jean-Mistral, C., Sylvestre, A., Basrour, S., and Chaillout, J.-J., 2010, "Dielectric Properties of Polyacrylate Thick Films Used in Sensors and Actuators," Smart Mater. Struct., **19**(7), p. 075019.
[13] Qiang, J., Chen, H., and Li, B., 2012, "Experimental Study on the Dielectric Properties of Polyacrylate Dielectric Elastomer," Smart Mater. Struct., **21**(2), p. 025006.
[14] Zhang, Q. M., Hengfeng, L., Poh, M., Xia, F., Cheng, Z. -Y., Xu, H., and Huang, C., 2002, "An All-Organic Composite Actuator Material With High Dielectric Constant," Nature, **419**, pp. 284–287.
[15] Huang, C., and Zhang, Q., 2004, "Enhanced Dielectric and Electromechanical Responses in High Dielectric Constant All-Polymer Percolative Composites," Adv. Funct. Mater., **14**(5), pp. 501–506.
[16] Huang, C., Zhang, Q. M., Li, J. Y., and Rabeony, M., 2005, "Colossal Dielectric and Electromechanical Responses in Self-Assembled Polymeric Nanocomposites," Appl. Phys. Lett., **87**(18290), pp. 1.
[17] Carpi, F., and De Rossi, D., 2005, "Improvement of Electromechanical Actuating Performances of a Silicone Dielectric Elastomer by Dispersion of Titanium Dioxide Powder," IEEE Trans. Dielectric. Electric. Insulation, **12**(4), pp. 835–843.
[18] Zhang, S., Huang, C., Klein, R. J., Xia, F., Zhang, Q. M., and Cheng, Z.-Y., 2007, "High Performance Electroactive Polymers and Nano-Composites for Artificial Muscles," J. Intell. Mater. Syst. Struct., **18**(2), pp. 133–145.
[19] Meddeb, A. M., and Ounaies, Z., 2012, "Nano-Enhanced Polymer Composites for Energy Storage Applications," Proc. SPIE 8342, Behavior and Mechanics of Multifunctional Materials and Composites 2012, **8342**.
[20] Liu, H., Zhang, L., Yang, D., Yu, Y., Yao, L., and Tian, M., 2013, "Mechanical, Dielectric, and Actuated Strain of Silicone Elastomer Filled With Various Types of TiO_2," Soft Mater., **11**(3), pp. 363–370.
[21] Pan, C., Markvicka, E. J., Malakooti, M. H., Yan, J., Hu, L., Matyjaszewski, K., and Majidi, C., 2019, "A Liquid-Metal–elastomer Nanocomposite for Stretchable Dielectric Materials," Adv. Mater., **31**(23), p. 1900663.
[22] Lopez-Pamies, O., 2014, "Elastic Dielectric Composites: Theory and Application to Particle-Filled Ideal Dielectrics," J. Mech. Phys. Solids, **64**, pp. 61–82.
[23] Keip, M. A., Steinmann, P., and Schröder, J., 2014, "Two-Scale Computational Homogenization of Electro-Elasticity At Finite Strains," Comput. Methods Appl. Mech. Eng., **278**, pp. 62–79.
[24] Miehe, C., Vallicotti, D., and Teichtmeister, S., 2016, "Homogenization and Multiscale Stability Analysis in Finite Magneto-Electro-Elasticity. Application to Soft Matter EE, ME and MEE Composites," Comput. Methods Appl. Mech. Eng., **300**, pp. 294–346.
[25] Pelteret, J.-P., Davydov, D., McBride, A., Vu, D. K., and Steinmann, P., 2016, "Computational Electro-Elasticity and Magneto-Elasticity for Quasi-Incompressible Media Immersed in Free Space," Int. J. Numer. Methods Eng., **108**, pp. 1307–1342.
[26] Lefèvre, V., and Lopez-Pamies, O., 2017, "Nonlinear Electroelastic Deformations of Dielectric Elastomer Composites: I—Ideal Elastic Dielectrics," J. Mech. Phys. Solids, **99**, pp. 409–437.
[27] Lefèvre, V., and Lopez-Pamies, O., 2017, "Nonlinear Electroelastic Deformations of Dielectric Elastomer Composites: II—non-Gaussian Elastic Dielectrics," J. Mech. Phys. Solids, **99**, pp. 438–470.
[28] Ghosh, K., and Lopez-Pamies, O., 2020, "On the Two-Potential Constitutive Modeling of Dielectric Elastomers," Meccanica.
[29] Dorfmann, A., and Ogden, R. W., 2005, "Nonlinear Electroelasticity," Acta Mech., **174**, pp. 167–183.
[30] Suo, Z., Zhao, X., and Greene, W. H., 2008, "A Nonlinear Field Theory of Deformable Dielectrics," J. Mech. Phys. Solids., **56**(2), pp. 467–486.
[31] Treloar, L. R. G., 1944, "The Elasticity of a Network of Long-chain Molecules. II," Rubber Chem. Technol., **17**(2), pp. 296–302.
[32] Arruda, E. M., and Boyce, M. C., 1993, "A Three-Dimensional Constitutive Model for the Large Stretch Behavior of Rubber Elastic Materials," J. Mech. Phys. Solids, **41**(2), pp. 389–412.
[33] Gent, A. N., 1996, "A New Constitutive Relation for Rubber," Rubber Chem. Technol., **69**(1), pp. 59–61.
[34] Lopez-Pamies, O., 2010, "A New I1-based Hyperelastic Model for Rubber Elastic Materials," C. R. Mécanique, **338**(1), pp. 3–11.
[35] Kittel, C., McEuen, P., and McEuen, P., 1976, *Introduction to Solid State Physics*, Vol. 8, Wiley, New York.
[36] Tian, L., Tevet-Deree, L., and Bhattacharya, K., 2012, "Dielectric Elastomer Composites," J. Mech. Phys. Solids, **60**(1), pp. 181–198.
[37] Toupin, R. A., 1956, "The Elastic Dielectric," J. Ration. Mech. Anal., **5**(6), pp. 849–915.
[38] Spinelli, S. A., Lefèvre, V., and Lopez-Pamies, O., 2015, "Dielectric Elastomer Composites: A General Closed-Form Solution in the Small-Deformation Limit," J. Mech. Phys. Solids, **83**, pp. 263–284.
[39] Lefèvre, V., and Lopez-Pamies, O., 2014, "The Overall Elastic Dielectric Properties of a Suspension of Spherical Particles in Rubber: An Exact Explicit Solution in the Small-Deformation Limit," J. Appl. Phys., **116**(13), p. 134106.
[40] Talbot, D. R. S., and Willis, J. R., 1985, "Variational Principles for Inhomogeneous Nonlinear Media," IMA J.Appl. Math., **35**(1), pp. 39–54.
[41] Lopez-Pamies, O., Goudarzi, T., and Danas, K., 2013, "The Nonlinear Elastic Response of Suspensions of Rigid Inclusions in Rubber: II — A Simple Explicit Approximation for Finite-Concentration Suspensions," J. Mech. Phys. Solids, **61**(1), pp. 19–37.
[42] Fassler, A., and Majidi, C., 2015, "Liquid-Phase Metal Inclusions for a Conductive Polymer Composite," Adv. Mater., **27**(11), pp. 1928–1932.
[43] Hossain, M., Vu, D. K., and Steinmann, P., 2012, "Experimental Study and Numerical Modelling of VHB 4910 Polymer," Comput. Mater. Sci., **59**, pp. 65–74.
[44] Kumar, A., and Lopez-Pamies, O., 2016, "On the Two-Potential Constitutive Modeling of Rubber Viscoelastic Materials," Comptes Rendus Mecanique, **344**(2), pp. 102–112.
[45] Lefèvre, V., and Lopez-Pamies, O., 2017, "Homogenization of Elastic Dielectric Composites With Rapidly Oscillating Passive and Active Source Terms," SIAM J. Appl. Math., **77**(6), pp. 1962–1988.